Controls on spatial variations in flow resistance along steep mountain streams

Gabrielle C. L. David,[1] Ellen Wohl,[1] Steven E. Yochum,[2] and Brian P. Bledsoe[2]

Received 17 April 2009; revised 9 September 2009; accepted 29 September 2009; published 12 March 2010.

[1] Detailed channel and water surface surveys were conducted on 15 mountain stream reaches (9 step-pool, 5 cascade, and 1 plane-bed) using a tripod-mounted Light Detection and Ranging scanner and laser theodolite. Reach-average velocities were measured at varying discharges with dye tracers and fluorometers. Multiple regressions and analysis of variance tests were used to test hypothesized correlations between Darcy-Weisbach friction coefficient, f, and potential control variables. Gradient (S_0) and relative grain submergence (R_h/D_{84}) individually explained a low proportion of the variability in f ($R^2 = 0.18$), where R_h is hydraulic radius, D_{84} is the 84th percentile of the cumulative grain size distribution, and R^2 is equal to the coefficient of determination. Because channel type, grain size, and S_0 are interrelated, we tested the hypothesis that f is highly correlated with all three of these variables or a combination of the above variables with flow period (a categorical variable) or dimensionless unit discharge (q^*). Total resistance correlated strongly (adj-R^2 = 0.74, 0.69, and 0.64) with S_0, flow period, wood load (volume of wood/m^2 of channel), q^*, and channel type (step-pool, cascade, plane-bed). Total resistance differed between step-pool and plane-bed and between cascade and plane-bed reaches. Significant differences in f in step-pool and cascade reaches were found at the same values of flow and S_0. The regression analyses indicate that discharge explains the most variability in f, followed by S_0 when discharge is similar among channel reaches, but that R_h/D_{84} is not an appropriate variable in these steep mountain streams to represent variations in both resistance and discharge. Results also indicate that the forms of resistance among channel types are sufficiently different to change the relationship of the control variables with f in each channel type. These results can be used to further the development of predictive equations for high-gradient mountain streams.

Citation: David, G. C. L., E. Wohl, S. E. Yochum, and B. P. Bledsoe (2010), Controls on spatial variations in flow resistance along steep mountain streams, *Water Resour. Res.*, *46*, W03513, doi:10.1029/2009WR008134.

1. Introduction

[2] Gradient is a defining characteristic of any stream channel. Gradient coupled with flow governs the amount of energy available for transporting material or eroding the banks and bed. Reach-scale gradient can be an independent variable in mountain streams and typically correlates well with channel morphology [*Montgomery and Buffington*, 1997; *Wohl and Merritt*, 2005] and with grain size [*Wohl et al.*, 2004].

[3] Energy is dissipated in channels through resistance to flow from interactions with the bed and banks and formation of waves at the free surface [*Bathurst*, 1982]. In low-gradient channels, resistance to flow and subsequent dissipation of energy occur when water is forced around channel bends or over bed forms such as ripples and dunes and from grain resistance. High-gradient mountain streams dissipate energy when water flows over poorly sorted grains in the bed and banks and over bed forms such as steps and pools, creating a constant alternation between supercritical and subcritical flow and causing energy dissipation through hydraulic jumps. Mountain streams differ from their low-gradient counterparts by having large boulders that are of the same order of magnitude as the depth of flow, low values of relative grain submergence (R_h/D_{84}, where R_h is hydraulic radius and D_{84} is the 84th percentile of the cumulative grain size distribution), armored beds, and wood that commonly spans the entire width of the channel [*Bathurst*, 1993; *Wohl*, 2000].

[4] The effect of gradient on flow velocity and resistance is expressed in the three primary resistance equations developed by Chezy, by Darcy and Weisbach, and by Manning:

$$V = C(R_h S_f)^{1/2} = \left(\frac{8gR_h S_f}{f}\right)^{1/2} = \frac{R_h^{2/3} S_f^{1/2}}{n} \qquad (1)$$

where V is mean flow velocity (m/s); C is Chezy coefficient; R_h is hydraulic radius (m); S_f is friction slope (m/m); f is

[1]Department of Geosciences, Colorado State University, Fort Collins, Colorado, USA.
[2]Department of Civil and Environmental Engineering, Colorado State University, Fort Collins, Colorado, USA.

0043-1397/10/2009WR008134

Darcy-Weisbach friction factor; g is acceleration due to gravity (m/s^2); and n is Manning coefficient. The coefficients in each of these equations express the total resistance to flow. For the remainder of this paper we will focus on the Darcy-Weisbach equation and use f to express total flow resistance because it is nondimensional and is physically interpretable as a drag coefficient if resistance is equated with gravitational driving forces per unit bed area [*Ferguson*, 2007].

[5] One difficulty in quantifying the flow resistance in mountain streams is that V, R_h, and S_f exhibit large spatial and temporal variability. Many empirical equations have been developed that relate f to these and other channel variables, but these typically perform poorly when extrapolated to other steep channels and in some cases have been shown to have errors as high as 66% [*Bathurst*, 1985, 1986, 2002; *Wohl*, 2000; *Katul et al.*, 2002; *Aberle and Smart*, 2003; *Curran and Wohl*, 2003; *Ferguson*, 2007].

[6] Part of the uncertainty in applying empirically based equations to new sites is that the relative importance of different sources of resistance can vary between sites. Total resistance is typically partitioned into grain (form drag on individual particles and viscous/skin friction on their surfaces), form (dunes, bars, steps), and spill (flow transitions and wave drag on elements protruding above the water surface) resistance [*Einstein and Barbarossa*, 1952; *Parker and Peterson*, 1980; *Wilcox et al.*, 2006; *Ferguson*, 2007]. The contribution made by each of these sources of resistance can differ in relation to gradient, channel morphology, or other factors [*Ferguson*, 2007]. Previous studies have typically focused on quantifying and/or partitioning resistance within a particular channel morphology [*Lee and Ferguson*, 2002; *Wilcox and Wohl*, 2007; *Comiti et al.*, 2007, 2009; *Reid and Hickin*, 2008]. We propose that because gradient is such an important influence on form and process in steep channels, spatial patterns of relative total resistance in mountain streams vary consistently in relation to gradient and thus channel morphology.

[7] The morphology of mountain streams is typically characterized as cascade, step-pool, and plane-bed [*Grant et al.*, 1990; *Montgomery and Buffington*, 1997]. Cascades form at $S_0 > 0.06$ m/m (where S_0 is bed gradient) and are characterized by tumbling flow over large, randomly arranged clasts [*Montgomery and Buffington*, 1997] that can create substantial grain resistance, dependent on stage. Skin friction and form drag around individual grains dissipate much of the mechanical energy. Occasional steps may be found in cascade reaches creating a limited amount of spill resistance.

[8] Step-pool channels form at gradients of $0.03 < S_0 < 0.10$ m/m [*Montgomery and Buffington*, 1997]. These reaches alternate between supercritical flow over steps transverse to flow and plunge pools with subcritical flow [*Zimmermann and Church*, 2001; *Church and Zimmermann*, 2007]. Steps create flow resistance by skin friction over large particles and wood, form drag from pressure differences around the upstream and downstream sides of an object, and spill resistance created from flow acceleration and deceleration. The total resistance in step-pool channels is dominated by spill resistance, which varies with wood amount and location [*Curran and Wohl*, 2003; *Wilcox et al.*, 2006; *Comiti et al.*, 2009]. *Comiti et al.* [2008] found that the presence of wood dams in the southern Andes can increase flow resistance up to one order of magnitude.

[9] Plane-bed channels lack well-defined, rhythmically occurring bed forms and occur at gradients of 0.01 to 0.03 m/m. This channel type is considered a transition between supply limited cascade and step-pool reaches and transport-limited pool riffle reaches [*Montgomery and Buffington*, 1997; *Wohl*, 2000]. The bed surface of the plane-bed reach is armored and has a threshold mobility near bankfull [*Montgomery and Buffington*, 1997].

[10] Previous studies have demonstrated that discharge exerts an important influence on resistance; at-a-site variation in f can be up to 100% as discharge and flow depth vary [*Lee and Ferguson*, 2002; *Reid and Hickin*, 2008]. Some investigators incorporate a measure of discharge such as R_h [*Jarrett*, 1984], discharge per unit width, q [*Bjerklie et al.*, 2005], or dimensionless unit discharge, $q^* = q/\sqrt{gD_{84}^3}$ [*Comiti et al.*, 2007; *Ferguson*, 2007]; others use a ratio of flow depth to boundary roughness such as relative submergence of grains (R_h/D_{84}) or relative submergence of the bed (R_h/s_{bed}) where s_{bed} is equal to the standard deviation of the bed elevation [*Aberle and Smart*, 2003]. *Bathurst* [1985], for example, characterized roughness based on the relative grain submergence value as large-scale ($0 < R_h/D_{84} < 1$), intermediate-scale ($1 < R_h/D_{84} < 4$), or small-scale ($R_h/D_{84} > 4$), and *Ferguson* [2007] proposed resistance equations with different parameters for deep and shallow flows. On the basis of this, we also propose that spatial patterns of relative total resistance in mountain streams vary consistently in relation to discharge, expressed via relative submergence of grains, steps, and the bed.

[11] To improve predictions of resistance and estimation of discharge, it is important to obtain a better understanding of resistance throughout a channel network, including variations in resistance within each type of channel morphology. Our primary objective is to understand how resistance varies with gradient, channel morphology, and relative submergence of grains, steps, and the bed throughout a channel network. We hypothesize that predictable patterns of relative magnitude of total resistance exist throughout a channel network and that simple variables such as gradient can be used to predict these patterns. Because each morphologic type of cascade, step-pool, and plane-bed spans a range of values for gradient and grain size, our secondary objective is to examine how resistance varies with gradient, relative grain submergence, and discharge within each channel type. This objective reflects our understanding that the influence of each variable on total resistance may differ based on gross morphology differences within each channel type.

[12] We address the first objective by testing two hypotheses with respect to flow resistance across a channel network. The null hypotheses are not explicitly listed for any of the hypotheses expressed below. H1: Total resistance correlates most strongly with a combination of potential control factors, which include S_0, R_h/D_{84}, q^*, R_h/s_{bed}, wood load (m^3/m^2), and the categorical variables flow period and channel type, rather than with any single potential control factor. Relative grain submergence, q^*, R_h/s_{bed}, and flow period all represent changes in discharge in each reach. Relative submergence of D_{84} and s_{bed} represent variations in discharge under the assumption that R_h changes with discharge, but D_{84} and s_{bed} remain relatively constant. An alternative hypothesis is H2: Total resistance correlates most strongly with a single variable. Both hypotheses test dif-

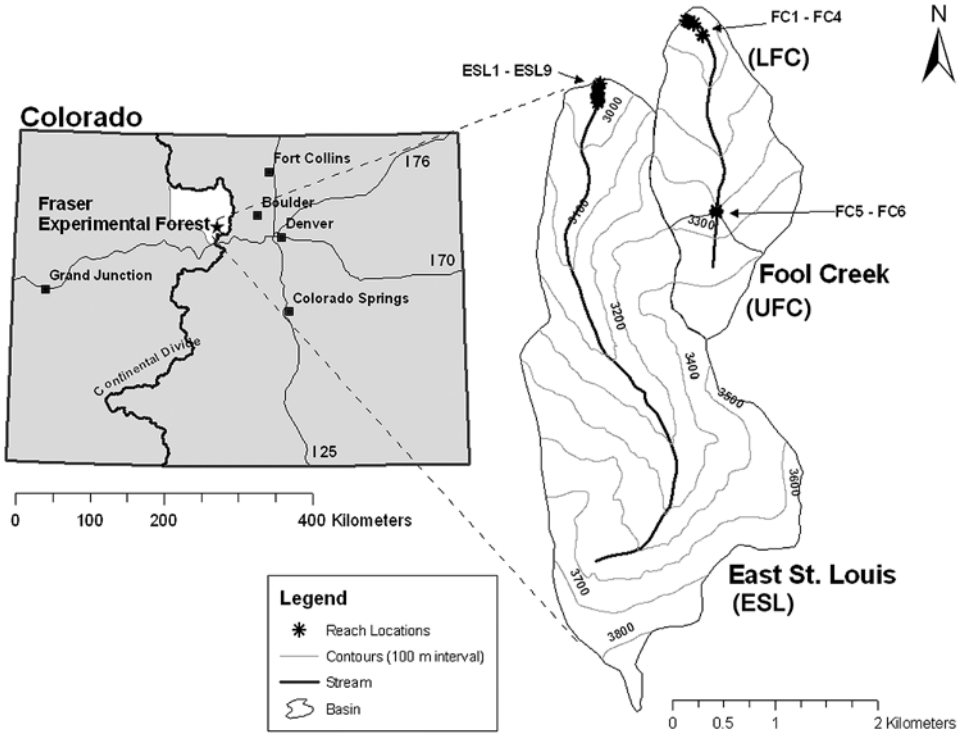

Figure 1. Location map of Fraser Experimental Forest.

ferences in *f* between sites rather than at-a-site. Our choice of potential control variables reflects past work in this research field [*Bathurst*, 2002; *Aberle and Smart*, 2003; *Wohl and Merritt*, 2005; *Comiti et al.*, 2007; *Ferguson*, 2007].

[13] We also address our second objective by testing three hypotheses with respect to resistance between channel types and resistance within each channel type. H3: For a given gradient, there is a consistent difference in total resistance between step-pool and cascade channels. This hypothesis reflects the fact that an overlap occurs in the gradient range at which each channel type can form and tests the possibility that channel morphology rather than gradient exerts the strongest influence on *f*. H4: For a given R_h/D_{84}, there is a consistent difference in total resistance between step-pool and cascade reaches. This hypothesis provides another means of examining the possibility that channel type exerts the strongest influence on *f*. H5: For each individual channel type, there is a consistent difference in which variables control variations in *f*. This final hypothesis reflects our understanding that total resistance in each channel type may result from grain, form, or spill resistance. The separate contributions from each of these components of resistance may result in different control variables being significantly related to total resistance in each channel type. For instance, in step-pool reaches the relationship between relative step submergence (R/H, where H is step height) and *f* is investigated.

2. Field Area

[14] East St. Louis Creek (ESL) and Fool Creek are located in Fraser Experimental Forest in the Colorado Rockies 112 km west-northwest of Denver (Figure 1). Elevation varies from 3925 m above sea level (asl) at the top of the Fool Creek basin to 2895 m asl at the bottom of East St. Louis Creek (Table 1). The Fool Creek basin is subdivided into Lower Fool Creek (LFC) and Upper Fool Creek (UFC) (Figure 1). Vegetation varies from Engelmann spruce and subalpine fir at higher elevations to lodgepole pine at lower elevations. Alpine tundra can also be found at the higher elevations in both basins. Runoff is dominated by snowmelt with small contributions by summer convective storms [*Trayler and Wohl*, 2000]. Average annual precipitation over the entire forest is 787 mm (http://www.fs.fed.us/rm/fraser/about/index.shtml). Historically, peak discharges occur in mid-June, with 80% of the total flows occurring between April and October [*Wilcox and Wohl*, 2007].

Table 1. Drainage Basin Information

Drainage Basin Name	Drainage Area (km^2)	Elevation Range of Basin (m a.s.l.)	Number of Step-Pool Reaches	Number of Cascade Reaches	Number of Plane-Bed Reaches	Total Number of Reaches
ESL	8.73	2895 to 3850	5	3	1	9
LFC[a]	2.89	2910 to 3925	4	0	0	4
UFC	0.69	3212 to 3925	0	2	0	2

[a]The drainage area and elevation ranges include UFC.

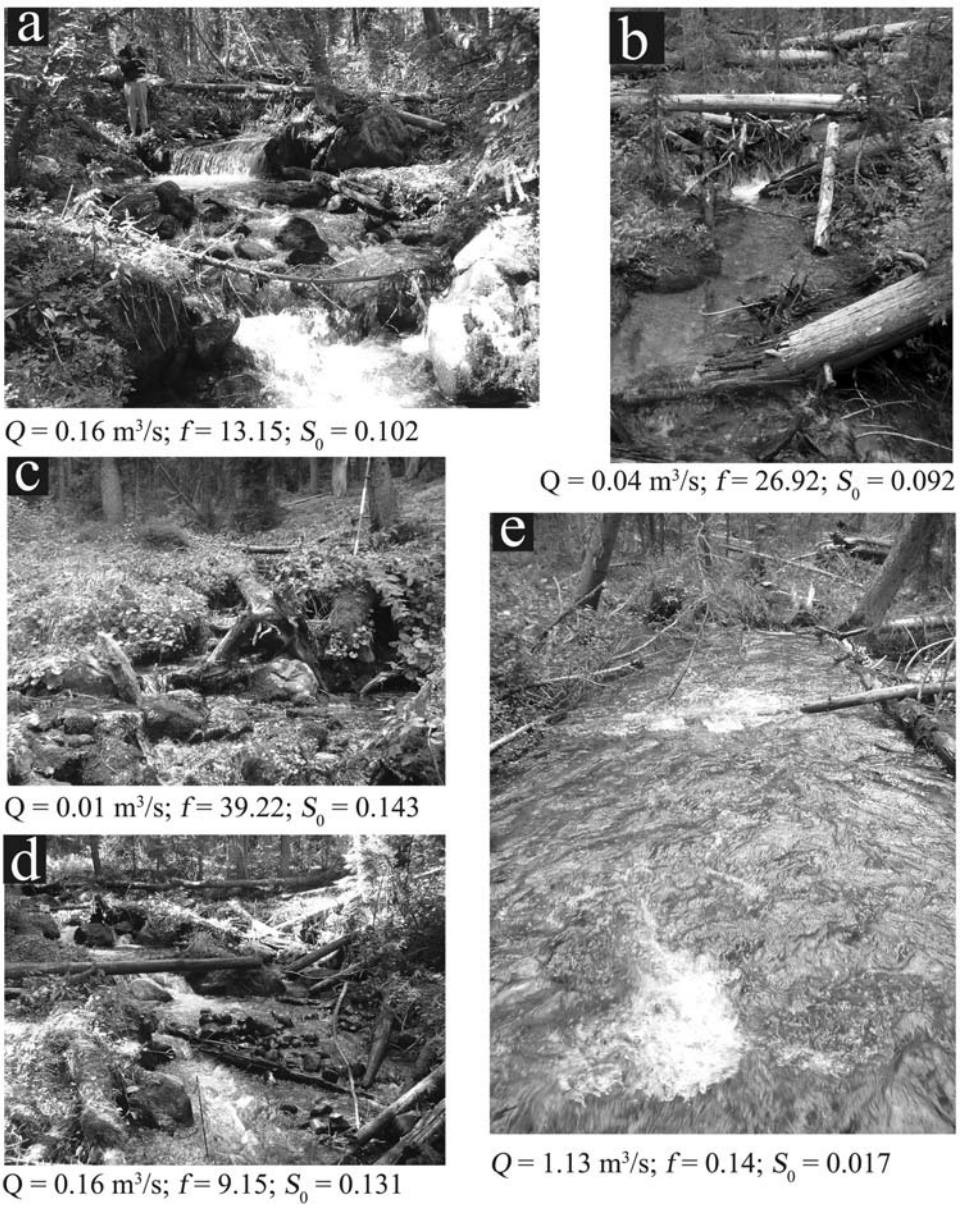

Figure 2. Photograph of a step-pool, cascade reach in each basin and the plane-bed reach in East St. Louis Creek. (a) Step-pool reach on East St. Louis Creek (ESL4) during August 2007 survey; (b) step-pool reach on Lower Fool Creek (FC3) during July 2008 survey; (c) cascade reach on Upper Fool Creek (FC5) during August 2007 survey; (d) cascade reach on East St. Louis (ESL3) during August 2007 survey; (e) plane-bed reach on East St. Louis (ESL6) during June 2008 survey.

[15] Each creek is in a confined valley surrounded by Pleistocene and Holocene lateral moraines and underlain by pre-Cambrian biotite schist and gneiss and Silver Plume granite [*Taylor*, 1975]. Both basins have shallow soils with low silt/clay content that are mainly derived from gneiss and schist (http://www.fs.fed.us/rm/fraser/about/index.shtml).

[16] ESL drains approximately 8.73 km^2 and has been gauged since 1943. LFC, including UFC, drains 2.89 km^2 and has been gauged since 1941. UFC is a 0.69 km^2 basin with a gauge installed around 1986. All of the basins are dominated by cascade and step-pool morphologies above the gauges, with limited plane-bed reaches (Table 1).

[17] Step-pool reaches in both ESL and LFC include large amounts of wood (Figure 2). Over 95% of the wood in the step-pool reaches is found in the steps. ESL4 and FC1 are the only two step-pool reaches where 100% of the steps are boulder steps. The rest of the step-pool reaches are more varied, with half the steps being boulder steps and the other half having steps created by a wood jam around one large keystone boulder. FC3 is the only reach where all the steps are wood steps. The cascade reaches in both basins contain a small number of steps and except for ESL5 these steps are mainly boulder steps. These reaches are still identified as cascade since the pools are not as wide as channel and the majority of the reach has tumbling flow over large boulders [*Zimmermann and Church*, 2001]. In ESL3 and ESL8, large bars of boulders, wood, and herbaceous vegetation existed above the mean annual peak flow line in the middle of the

Table 2. Average Values for Reach Dimensions and Hydraulic Variables for the Four Flow Periods in Each Reach[a]

Reach	Channel Type	L_r (m)	S_0 (m/m)	A (m^2)	R (m)	H/L_s	D_{50} (m)	D_{84} (m)	V (m/s)	Q (m^3/s)	q^* (m/s)	Fr	Re	f
ESL1	step-pool	27.3	0.086	0.29	0.12	0.13	0.05	0.16	0.22	0.06	0.16	0.21	2.2E+04	4.23
		31.6	0.104	0.99	0.25	0.18			0.66	0.66	1.16	0.42	1.5E+05	16.32
ESL2	step-pool	13.7	0.085	0.45	0.15	0.14	0.01	0.07	0.25	0.11	0.76	0.20	3.4E+04	4.35
		14.7	0.095	1.00	0.25	0.20			0.63	0.63	3.34	0.42	1.4E+05	16.84
ESL3	cascade	10.1	0.124	0.42	0.14	0.31	0.06	0.13	0.39	0.16	0.46	0.33	4.8E+04	3.75
		11.3	0.140	0.87	0.18	0.66			0.73	0.64	1.18	0.55	1.2E+05	9.15
ESL4	step-pool	15.6	0.102	0.50	0.17	0.19	0.07	0.17	0.54	0.16	0.31	0.25	5.0E+04	5.17
		16.5	0.128	0.99	0.26	0.24			0.73	0.68	1.05	0.43	1.6E+05	13.15
ESL5	cascade	12.5	0.136	0.59	0.15	0.21	0.05	0.14	0.25	0.15	0.26	0.21	3.3E+04	10.66
		15.1	0.160	1.20	0.24	1.03			0.52	0.63	0.90	0.34	1.1E+05	22.85
ESL6	plane-bed	5.9	0.017	0.44	0.15	N/A	0.02	0.09	0.42	0.18	0.88	0.35	5.5E+04	0.10
		6.5	0.023	0.89	0.26				2.07	1.85	7.92	1.30	3.8E+05	1.31
ESL7	cascade	22.1	0.083	0.42	0.15	N/A	0.08	0.17	0.43	0.18	0.33	0.35	5.7E+04	3.34
		24.3	0.099	0.97	0.25				0.73	0.71	1.04	0.46	1.6E+05	5.26
ESL8	step-pool	30.7	0.082	0.48	0.16	0.07	0.07	0.17	0.36	0.17	0.30	0.29	5.1E+04	4.22
		35.5	0.099	0.91	0.23	0.09			0.62	0.57	0.80	0.41	1.3E+05	8.05
ESL9	step-pool	16.1	0.095	0.47	0.17	0.14	0.06	0.15	0.34	0.16	0.38	0.26	5.0E+04	5.60
		18.6	0.117	0.92	0.25	0.18			0.62	0.57	1.09	0.40	1.4E+05	10.78
FC1	step-pool	22.3	0.058	0.09	0.06	0.06	0.03	0.08	0.20	0.02	0.18	0.25	1.1E+04	1.07
		25.1	0.062	0.38	0.16	0.08			0.86	0.33	2.18	0.68	1.2E+05	7.58
FC2	step-pool	14.2	0.071	0.08	0.06	0.06	0.03	0.08	0.19	0.01	0.18	0.25	1.0E+04	2.23
		15.1	0.077	0.39	0.18	0.11			0.68	0.26	2.21	0.52	1.0E+05	9.59
FC3	step-pool	11.9	0.079	0.12	0.07	0.09	0.01	0.05	0.11	0.01	0.28	0.13	6.9E+03	7.24
		14.9	0.095	0.55	0.19	0.15			0.43	0.24	3.27	0.32	7.2E+04	42.13
FC4	step-pool	18.9	0.130	0.14	0.09	0.11	0.05	0.10	0.15	0.02	0.19	0.16	1.2E+04	3.82
		19.8	0.136	0.49	0.20	0.17			0.75	0.37	2.42	0.53	1.3E+05	39.89
FC5	cascade	11.9	0.143	0.05	0.05	0.33	0.03	0.09	0.12	0.01	0.10	0.17	5.5E+03	4.64
		14.2	0.163	0.20	0.13	0.86			0.60	0.12	1.32	0.54	6.6E+04	39.22
FC6	cascade	19.1	0.166	0.04	0.05	0.21	0.05	0.09	0.13	0.01	0.09	0.19	5.7E+03	4.73
		22.1	0.195	0.17	0.12	0.30			0.61	0.10	1.06	0.58	6.2E+04	36.16

[a]Abbreviations are thalweg length, L_r, gradient, S_0, average cross-sectional area, A, average hydraulic radius, R_h, step steepness, H/L_s, particle size, D_{50} and D_{84}, average velocity, V, average discharge, Q, dimensionless unit discharge, q^*, Froude number, Fr, Reynolds number, Re, and Darcy-Weisbach friction factor, f. Values on top are minimum values and values on bottom are maximum values over the four flow periods. A minimum slope value does not necessarily correlate with a minimum f value. See Appendix A for full table.

reach, separating the flow into two paths. In ESL2, ESL5, and FC3 have a large and complex wood jam that causes a greater deceleration of the water than in other reaches and deposition of a relatively large amount of fine sediment just upstream of the step. ESL6, the lone plane-bed reach (Figure 2), can be found just upstream of the large wood step at the upstream end of ESL5.

3. Methods

3.1. Field Methods

[18] Fifteen channel reaches on East St. Louis Creek (ESL) and Fool Creek (FC) were selected in the field based on visual assessment of morphology (Table 2). Upper and lower boundaries of each reach were chosen to ensure consistent morphology and gradient within the reach. Reaches are labeled in order from downstream to upstream on each basin. A laser theodolite was used to collect bed and water surface data every 15 cm along the thalweg and banks of each reach. All measurements were made over two summers in 2007 and 2008. The water surface was surveyed during a high flow (June 2008), two intermediate flows (July 2007 and 2008), and one low flow (August 2007). These four measurement periods are referred to as flow periods in the rest of the paper and used as a categorical variable in the statistical analysis. The two intermediate flows are treated as separate flow periods. During each of these surveys the reach-averaged mean velocity was measured using Rhodamine WT dye tracer and fluorometers attached to rebar. The Rhodamine WT dye tracer was used in place of a salt tracer because of the requirements of the USDA Forest Service which administers the study site. The rebar were fixed in the thalweg of the streambed at the upstream and downstream end of each reach. The fluorometers were placed at 0.6 of the water depth (h) for each measurement. Previous studies have shown that despite the lack of a logarithmic velocity profile, the reach-averaged mean velocity can still be approximated by placing probes at $0.6h$ or $0.2h$ and $0.8h$ [*Wiberg and Smith*, 1991; *Legleiter et al.*, 2007; *Wilcox and Wohl*, 2007]. The probes recorded values at 1 s intervals and continued to record until the values returned to background levels. The measurements were repeated four times in each reach. The differences between the centroids of the mass of dye were used rather than the difference between peaks for determining the time difference between the two probes [*Lee and Ferguson*, 2002; *Curran and Wohl*, 2003]. The centroid method was preferred because large amount of noise in some of the measurements made a peak arrival time difficult to read. Also, previous researchers have found that peak times may vary based on reach length, whereas the centroid method is more consistent [*Calkins and Dunne*, 1970]. During the June 2008 survey, water was observed overbank in localized sections of a few reaches in both basins and new wood was found in two other reaches.

[19] A *Wolman* [1954] pebble count of 300 pebbles was conducted to determine particle size distribution in each reach. Usually, 100 pebbles are counted in a Wolman pebble count, but it has been shown that increasing the sample size

Figure 3. Example of the results of a LIDAR scan of ESL9. The arrow is pointing to the same log on (left) the photograph and (right) the point cloud. The photograph and scan image are both showing a wood step in ESL9.

can reduce the error [*Thorne and Zevenbergen*, 1985]. The intermediate axis of each clast was measured with a ruler. Many of the largest boulders (0.5–1 m) were partly embedded; therefore, the length of the intermediate axis was approximated. The pebble counts were done at evenly spaced cross sections throughout the reach, which were anywhere from 0.5 to 1 m apart. Separate particle size distributions were not determined for the steps and pools and only a composite value was used for the reach. A pebble count was repeated in one step-pool, cascade, and plane-bed reach and average errors of 13, 8, and 4%, respectively, were determined for each channel type. A 13% error for step-pool reaches is well within the range of ±10% to ±20% reported by *Ferguson* [2007].

[20] A tripod-mounted Light Detection and Ranging (LIDAR) Leica HDS Scanstation was used during the August 2007 low-flow period to capture bank and bed topography (Figure 3). Each individual scan was merged within a tolerance of 1 cm at the control points. Figure 3 shows both a photograph and an example of the resulting point cloud of ESL9. The point cloud density varied substantially in each reach. The LIDAR scans were coupled with a feature-based survey with variable gridding that depended upon the underwater features, which was completed with a laser theodolite. The water surface data were imported into the scans and used together with cross sections created in Cyclone 5.8.1 [*Leica Geosystems*, 2008] using the LIDAR scans, to calculate channel geometry data, i.e., width (w), depth (h), hydraulic radius (R_h), cross-sectional area (A). Values of these variables were reach averages based on multiple cross sections. The cross sections were evenly spaced (0.5 to 1.5 m) in each reach depending on the reach length. The cross sections were surveyed in Cyclone 5.8.1 and then imported into Microsoft Excel. A spreadsheet was created that allowed calculation of channel geometry data after importing the water surface elevation for each flow period.

[21] The water surface slope (S_w) and bed slope (S_0) were calculated for each reach using a linear regression on the laser theodolite surveys. The S_w is used to calculate f and S_0 is used in the statistical analyses. The average percent difference between S_w and S_0 is 4.2%, with the highest percent difference in the plane-bed reach with an average difference of 22.9% over the four flow periods. The average percent difference in the step-pool and cascade reaches is 2.8 and 2.6%, respectively.

[22] The standard deviation of bed elevation (s_{bed}) was calculated using the residuals of a planar regression of the elevation on the northing and easting axes. The northing and easting axes were taken from the laser theodolite survey of the thalweg. The relative step submergence, R_h/H, where H is step height, was calculated for step-pool reaches from thalweg and LIDAR data. The ratio of step steepness to gradient $(H/L_s)/S_0$ was also measured using the same data (where L_s is step length). Table 2 lists the minimum and maximum values for a selection of variables, which changed as a function of discharge, for each reach. Table 2 is presented to show the range of values that exist in each reach, but the minimum values in each row do not necessarily all correspond to each other; therefore, the full data set is shown in Appendix A.

[23] Wood length and diameter was measured for each flow period using a combination of the LIDAR scans, a tin created of the water surface in Cyclone 5.8.1, and photographs. The wood volume was calculated from these measurements and divided by the plan area of the reach (L_r*w). The wood volume includes pieces of wood found as single unattached pieces in the reach as well as in the steps. ESL2 and FC3 were found to have the largest wood load of any of the reaches.

3.2. Statistical Methods

[24] Both regression analysis and analysis of variance (ANOVA) were used in the program R to investigate which independent variables significantly influence f [*Jongman et al.*, 1995; *Kutner et al.*, 2005; *R Core Development Team*, 2007]. Therefore, the major goal of this analysis and the results presented in Table 3 are not prediction and should not be used outside the range of values shown in Appendix A. The friction factor was used in the form of $(8/f)^{0.5}$ and related to gradient, relative grain submergence, and channel type. The function, $(8/f)^{0.5}$, is easily related to dimensionless velocity (V/u*), where u* is shear velocity $(ghS_f)^{1/2}$, and the two other flow resistance coefficients,

$$\left(\frac{8}{f}\right)^{1/2} = \frac{C}{g^{1/2}} = \frac{R^{1/6}}{ng^{1/2}} \tag{2}$$

[*Bathurst*, 1985; *Thorne and Zevenbergen*, 1985]. The only time the friction factor is used in its regular form, as f, is when

Table 3. Linear Regressions of $(8/f)^{0.5}$ and f Versus Independent Variables and Categorical Variables[a]

	Independent Variables[b]	Model 1[c]	Model 2	Model 3	Model 4a	Model 4b	Model 5a	Model 5b	Model 6	Model 7	Model 8	Model 9	Model 10	Model 11	Model 12
Hypothesis		H1	H1	H1	H1	H1	H1	H2	H2	H2	H2	H2	H2[d]	H3	H4
Dependent variables[e]															
$(8/f)^{0.5}$	intercept	0.12*	0.17*	0.11*	0.22*	0.19*			0.89*	0.29*	0.88*		0.51*	0.23*	0.88
f	intercept						84.95*	242.64*				5.97*			
	S_0[f]	−0.63*	−0.66*	−0.89*	−0.69*	−0.45*	1.32*	0.79*		−0.54*				−0.69*	
	R/D_{84}				0.39*	0.56*					0.39*				0.41*
	q^*						−0.65*	−0.75*				−0.66*			
	R/s_{bed}								0.72*						
	wood load	−0.05*				−0.09*		0.13*					−0.10*		
	July 2007[g]	1.39*	1.46*	1.47*											
	July 2008[c]	1.36*	1.36*	1.38*											
	June 2008[c]	2.02*	2.10*	2.16*											
	August 2007[c]	1.00*	1.00*	1.0*											
	step-pool[h]			0.79*	0.76*	0.87	1.62*	1.09						0.86	0.98
	cascade			1.00*	1.00*	1.00	1.00*	1.00						1.00	1.00
	FC[i]		0.86*												
	ESL		1.00*												
F statistic		30.76	23.71	25.01	9.59	18.08	33.57	21.84	96.38	11.88	11.32	51.89	10.6	6.76	6.84
***p*-value**[j]		0.001	0.001	0.001	0.001	0.001	0.001	0.001	0.001	0.001	0.001	0.001	0.002	0.002	0.002
R^2		0.77	0.71	0.72	0.36	0.60	0.66	0.65	0.65	0.18	0.18	0.49	0.18	0.21	0.21
Adjusted R^2		0.74	0.68	0.69	0.32	0.57	0.64	0.62	0.64	0.17	0.16	0.49	0.16	0.18	0.18
Mallow C_p			10.04	8.16	56.23		12.47		58.52	82.29	82.83	25.66		79.92	84.79

[a]Models 1–4b, 6–8, and 10–12 use $(8/f)^{0.5}$ as the dependent variable. Models 5a–5b and 8 use f as the dependent variable. The numbers in each column under the model number show which variables were used in each regression. The Mallow's Cp is not shown for regressions that had outliers removed.
[b]Variables with asterisks indicate that value is significant at the $\alpha = 0.05$ level.
[c]FC3 Aug 2007 and FC3 July 2008 were both outliers when wood load is included in the regression. Therefore, both of these were removed.
[d]All ESL2 data were removed as outliers.
[e]Variables in bold were transformed using the natural log.
[f]Numbers shown are exponents of independent variables, if it is a categorical variable and that category is true than the number should be multiplied with the intercept.
[g]Part of Flow Period categorical variable with four levels that include July 2007, July 2008, June 2008, and August 2007.
[h]Part of Channel Type categorical variable that includes two levels in all models except for Model 7. The two levels are step-pool and cascade channel types.
[i]Part of drainage basin categorical variable that has two levels FC and ESL. FC includes both UFC and LFC.
[j]Where 0.001 is indicated, the value is actually <0.001.

it is used in a regression with q^*. The results of these regression models are presented so that they can be compared with the values calculated by *Comiti et al.* [2007]. The variables $(8/f)^{0.5}$, S_0, R_h/D_{84}, wood load, and q^* were log-transformed to meet regression assumptions of homoscedacity [*Jongman et al.*, 1995; *Kutner et al.*, 2005]. All regressions and variables were significant at an $\alpha = 0.05$ level.

[25] The plane-bed reach was removed as an outlier in the regression analysis and the ANOVA. Because there is only one plane-bed reach, it often drives the model by increasing the R^2 (coefficient of determination) value and causing heteroscedacity of the residuals. Therefore, the plane-bed reach is only included in the ANOVA testing the relationship between channel type and f, S_0, and R/D_{84}, respectively. A Tukey HSD method was used to gauge significant differences between means in the ANOVAs. The Tukey HSD method adjusts for differences in sample sizes, so appropriate comparisons can be made between means [*Kutner et al.*, 2005; *R Core Development Team*, 2007].

[26] Both the Mallow's C_p and adjusted R^2 were used to compare models. The C_p is calculated by comparing a reduced model to a model with all the variables. The minimum C_p is sought to determine the best model with the smallest mean squared error and the smallest bias [*Kutner et al.*, 2005]. The adjusted R^2 is adjusted for the number of variables in the model. The best model is associated with the maximum adjusted R^2 and all values reported in the results below are adjusted R^2. Flow period is used as a categorical variable because repeat measures were taken in the same reaches meaning that those values are not independent of each other. A benefit of using the categorical variable flow period is to understand how f varies at-a-site with discharge. To reduce autocorrelation, variables such as stream power, Froude number, and Reynolds number were not used in the analysis even though it is understood that each of these variables have an effect on f. Discharge (Q) is not included as a predictor of f since the ultimate goal of this type of research is to find variables that will help in prediction of f and subsequently Q and V in these high-gradient channels. We chose to include one variable, q^*, that includes Q in the calculation of the variable because of the success in using this variable from previous work on high-gradient streams and the understanding that the goal of some applications is to predict V when Q is known. It is also noted that in any regression models that include S_0 there may be issues with autocorrelation because of the collinearity between S_0 and S_w.

4. Results

4.1. Friction Factor, Gradient, Relative Submergence, Wood Load, Channel Type, and Drainage Basin (H1 and H2)

[27] H1 tests whether $(8/f)^{0.5}$ is significantly related to a combination of control variables which include S_0, R_h/D_{84},

q^*, wood load, flow period, and channel type. Table 3 shows seven models that combine S_0 with each flow variable (R_h/D_{84}, q^*, flow period) and channel type. The values in Table 3 for each of the continuous variables are all exponents that indicate the rate of change of each of the independent variable with the dependent variable. Gradient, R_h/D_{84}, q^*, flow period, and channel type all explain a significant amount of the variation in $(8/f)^{0.5}$ and f at the $\alpha = 0.05$ level. Gradient and channel type combined with either flow period or q^* are the models that explain the greatest amount of variability in both $(8/f)^{0.5}$ and f (Table 3). Models 3 and 5a have the highest adjusted R^2 (0.69 and 0.64) and lowest Mallow's C_p values (8.16 and 12.47). Models that include wood load (models 1, 4b, and 5b) also have an improved adjusted R^2. The rate of change of S_0 with $(8/f)^{0.5}$ varies between −0.45 and −0.89 for models 1 through 4b. As S_0 increases the value of $(8/f)^{0.5}$ decreases, indicating that f is highest at steeper gradients.

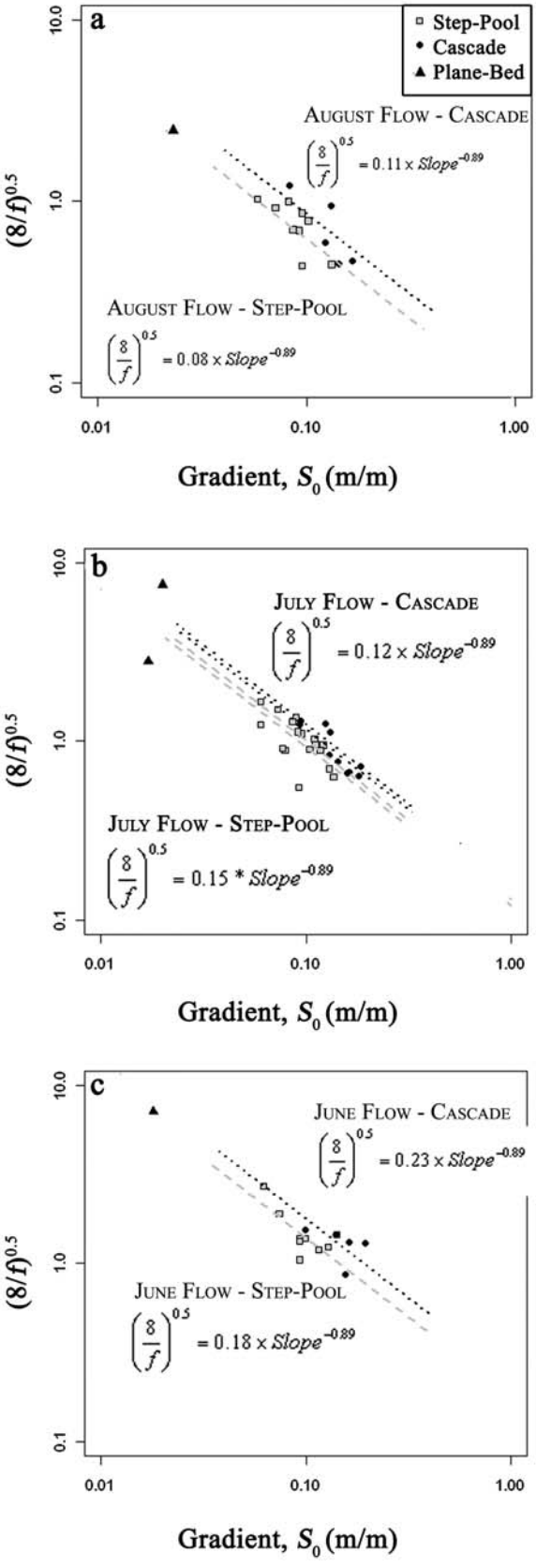

Figure 4. $(8/f)^{0.5}$ versus gradient (S_0) for each channel type, showing (a) trend line and points for August 2007 flow for cascade and step-pool channels, (b) trend lines and points for July 2007 and 2008 flows for cascade and step-pool channels, and (c) trend line and points for June 2008 flow for cascade and step-pool channels. The plane-bed reach is included in the plot but not in the regressions.

[28] Model 1 tests whether there is a consistent difference in $(8/f)^{0.5}$ for each flow period for a given S_0 and wood load. The model is improved with this categorical variable (adjusted $R^2 = 0.64$) and the intercepts for each flow period are significantly different from each other (Figure 4). Model 1 shows that for high-flow and intermediate-flow period, $(8/f)^{0.5}$ is significantly greater than August low-flow period (Table 3). Therefore, $(8/f)^{0.5}$ is lowest for the higher flows for a given S_0 and wood load. The interaction term between S_0 and flow period was tested but found to be not significant. Therefore, the rate of change of $(8/f)^{0.5}$ with S_0 is not significantly different at each flow period (Figure 4). If the rate of change was significantly different it would mean that the slope of the regression line is significantly different for each flow period. The relationship between $(8/f)^{0.5}$ and wood load was also found to be significant at a given S_0 and flow period. As wood load increases $(8/f)^{0.5}$ decreases. The interaction term was not significant between wood load and flow period; therefore, the rate of change does not vary with flow period.

[29] Model 2 tests whether there are significant differences in $(8/f)^{0.5}$ between the two basins, East St. Louis and Fool Creek, while holding gradient constant. The cascade reaches in UFC and step-pool reaches in LFC are combined in the Fool Creek basin. The two basins have some distinct characteristics relative to each other; therefore, we tested whether for a given S_0 there is a consistent difference in $(8/f)^{0.5}$ in East St. Louis versus Fool Creek, holding the flow period constant. The regression shows that there is a significant difference between the two (Table 3). For a given S_0 and flow period, $(8/f)^{0.5}$ in Fool Creek is higher than in East St. Louis. The interaction term between S_0 and drainage basin was found to be not significant. Therefore, the overall value of $(8/f)^{0.5}$ is affected by differences in each basin, but the rate of change of $(8/f)^{0.5}$ with S_0 is not affected by the basin. Because of the small number of reaches, it is not appropriate to also separate by channel type in the multiple regression, but the differences in $(8/f)^{0.5}$ between channel type and basin are further explored in the ANOVAs in section 4.4.

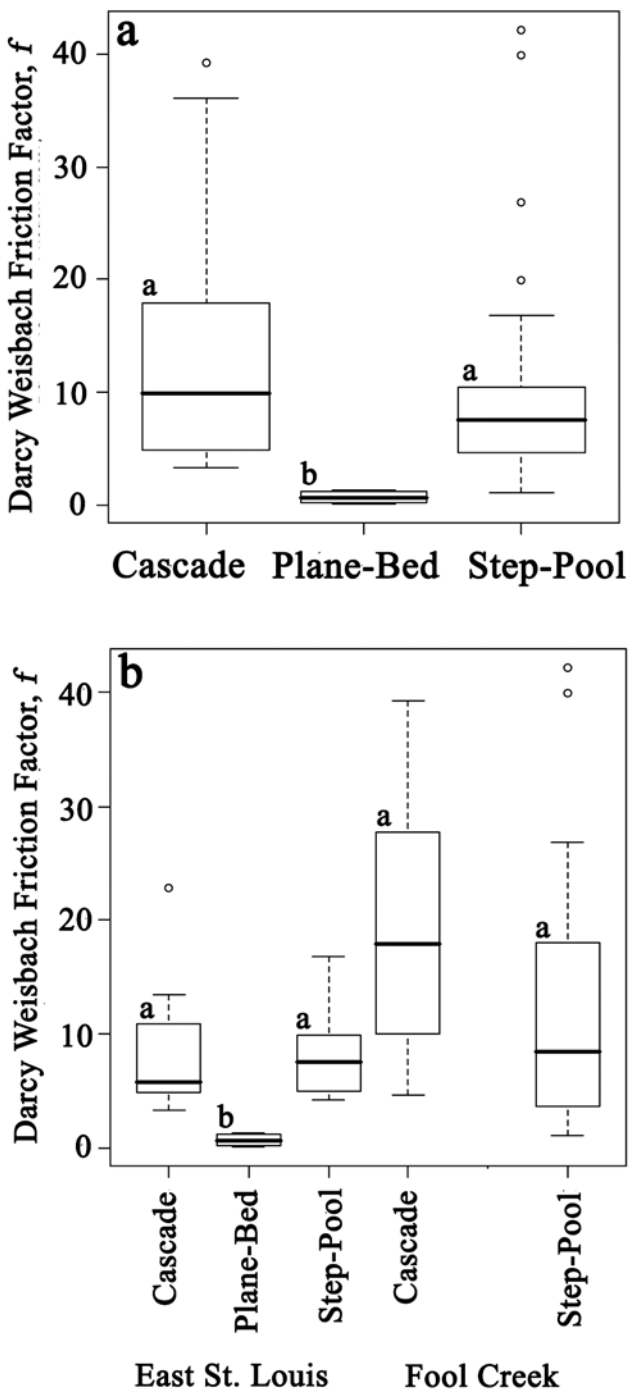

Figure 5. Box plots of (a) f versus channel type and (b) f versus channel type for each basin. The contrasting letters a and b above the boxes show the results of the significant ($p < 0.05$) pairwise differences in means from Tukey's test following an ANOVA. Box plots with the same letter do not have significantly different means; box plots with different letters do have significantly different means.

[30] The variation in $(8/f)^{0.5}$ between high and low flow is much greater in Fool Creek than in East St. Louis (Figure 5). Figure 5b displays the differences in the at-a-site variation in $(8/f)^{0.5}$ in both Fool Creek and East St. Louis. The greater variability in $(8/f)^{0.5}$ in Fool Creek is most likely related to the greater variation in flow depth and wetted width at the high versus low flows (Figure 6). The base flow remains much higher in East St. Louis after snowmelt than in Fool Creek. Therefore, the relatively small flow in Fool Creek has a much higher friction than the lowest surveyed flow in East St. Louis, causing an increased variability in $(8/f)^{0.5}$ in Fool Creek. Models 1 and 2 show that $(8/f)^{0.5}$ is correlated with S_0 throughout a channel network and that correlation is better explained by holding flow period and drainage basin constant.

[31] Models 5a and 5b show that f decreases as q^* increases while holding both S_0 and channel type constant. The dimensionless unit discharge is used in place of flow period and R_h/D_{84}. Wood load is included in model 5b, causing the channel type to no longer be significant. All variables (S_0, q^*, channel type) are found to explain a significant proportion of the variability in f while holding all other variables constant. The significance of q^* and improved model fits indicate that R_h/D_{84} does not completely encompass the effects of different flows in these steep mountain streams. The results shown in Table 3 therefore support H1; f correlates most strongly with a combination of potential control factors, rather than with any single potential control factor.

[32] The relationship between $(8/f)^{0.5}$ and individual control variables is shown with models 6 through 10 (Table 3). These models are shown to better understand the relationship between individual control variables and $(8/f)^{0.5}$ rather than between combinations of control variables and $(8/f)^{0.5}$. For all reaches at all flow periods, $(8/f)^{0.5}$ correlates positively with R_h/D_{84} and negatively with S_0. The relative grain submergence explains the same proportion of the variability in $(8/f)^{0.5}$ as does S_0 and wood load (models 7, 8, and 10). These results partially support the second hypothesis, that $(8/f)^{0.5}$ correlates with individual control variables (Table 3), but do not suggest that $(8/f)^{0.5}$ correlates most strongly with an individual control variable.

[33] The friction factor was found to be significantly related to q^*; as q^* increases, f decreases (model 9). In this case q^* is related to f rather than $(8/f)^{0.5}$. The relationship was found to explain more of the variability in f (adjusted $R^2 = 0.49$) than R/D_{84} (model 8, adjusted $R^2 = 0.16$). These results are reemphasized in model 4a, where S_0 combined with R_h/D_{84} and channel type explains a much smaller proportion of the variability in $(8/f)^{0.5}$ than a model with either flow period (model 4) or q^* (model 5). A model with wood load also explains a greater proportion of the variability, particularly when combined with S_0 and q^* or flow period. These results do not support H2 that f correlates most strongly with an individual variable. Therefore, the best model that explains the most variability in the data set is a model with a combination of control variables.

4.2. Friction Factor and Standard Deviation of Bed Elevation (H2)

[34] The D_{84}, D_{50}, Log(D_{84}/D_{50}), and s_{bed} were each regressed against velocity to determine which variable is the most appropriate roughness parameter. These roughness parameters are on the same order of magnitude as the flow depth, and the variation in each may be larger than the variation in flow depth. Therefore, it is expected that the individual roughness parameters would be related to flow velocity without accounting for flow depth. Both D_{84} and D_{50} were found to be significantly related to velocity, but no

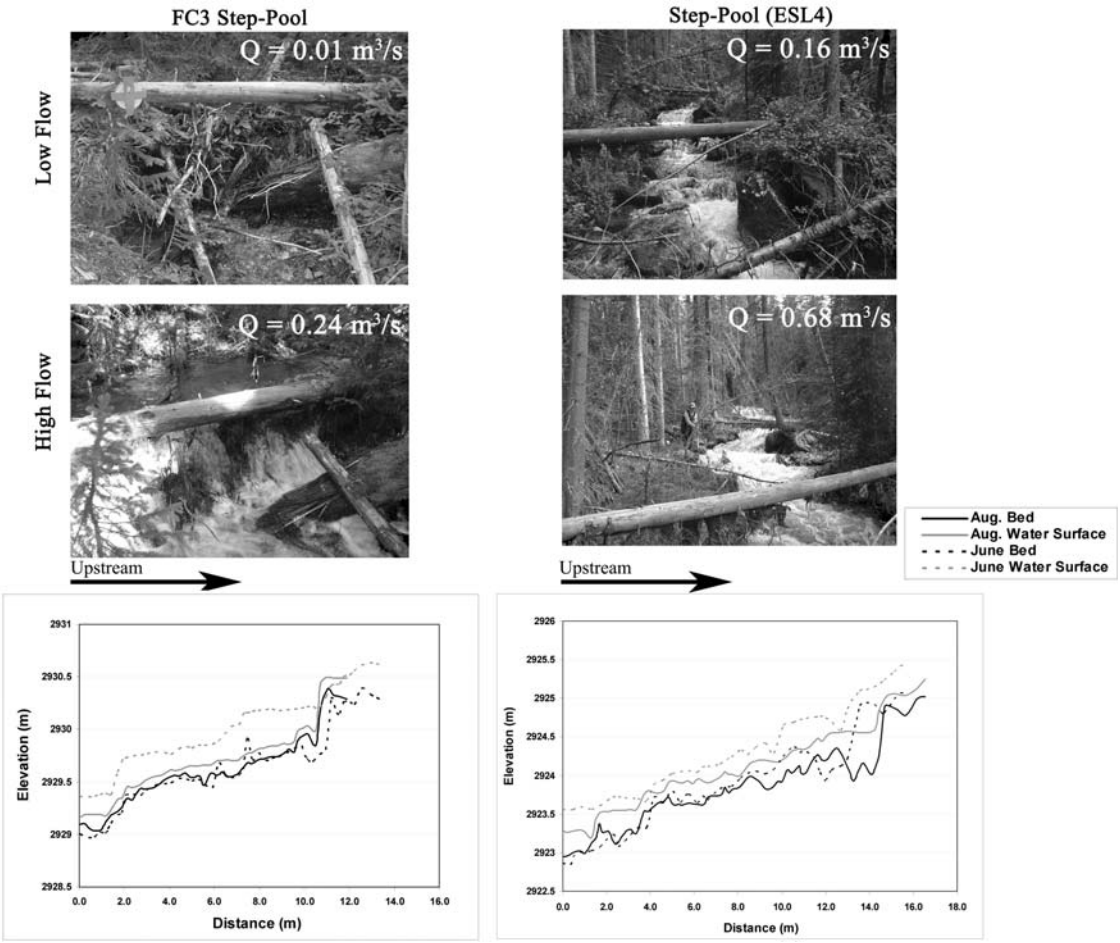

Figure 6. Comparison of the August 2007 (low) flow period and June 2008 (high) flow period in the step-pool reaches FC3 and ESL4. The longitudinal profiles are shown for each low-flow and high-flow survey for each reach. The photographs and graphs show the differences in depths and relative submergence at the two flows for each reach.

significant relationship could be found to exist between velocity and s_{bed} or velocity and Log(D_{84}/D_{50}). There is a significant relationship between R_h/s_{bed} and velocity, which is reflected in the significant relationship shown in model 6 between R_h/s_{bed} and $(8/f)^{0.5}$ (Table 3). R_h/s_{bed} as a relative submergence parameter explains more of the variation of $(8/f)^{0.5}$ than R_h/D_{84} (model 8). The improved relationship may result partially from the spurious correlation between R and $(8/f)^{0.5}$. The strong relationship supports the second hypothesis that $(8/f)^{0.5}$ correlates with R_h/s_{bed} despite the lack of correlation between s_{bed} and velocity.

4.3. Friction Factor and Channel Type (H2)

[35] Channel type, S_0, and grain size are all interrelated; therefore, we investigated how f varies by channel type. Figure 5 shows a box plot of the three channel types versus f, determined for the different flow periods. An ANOVA and a Tukey's test were used to compare significant differences between means of f. The friction factor was log transformed to meet normality assumptions of the ANOVA and Tukey's test. Means for cascade and step-pool channels were found to be significantly different from the plane-bed channel but not significantly different from each other. The Tukey HSD method takes account of the smaller sample size of 4 in the plane-bed versus 20 for the cascade and 35 for the step-pool reaches while gauging differences between means. How well this plane-bed reach represents plane-beds in mountain streams will be discussed further in a subsequent paper.

[36] Figure 5b shows the channel types separated by drainage basin. The box plot reemphasizes that the plane-bed reach is significantly different from all other channel types in both basins. The main differences between Fool Creek and East St. Louis are that the standard deviation of f is much broader for cascade and step-pool reaches in Fool Creek than in East St. Louis. Therefore, f does not vary significantly between cascade and step-pool reaches over all flow periods but does vary significantly between the cascade and plane-bed and between the step-pool and plane-bed reaches. Thus the results do not support hypothesis 2, that f correlates most strongly with individual control variable of channel type.

4.4. Friction Factor, Gradient, and Channel Type (H3)

[37] Figure 7 displays a significant variation in S_0 among channel types and among channel types in each basin. Once

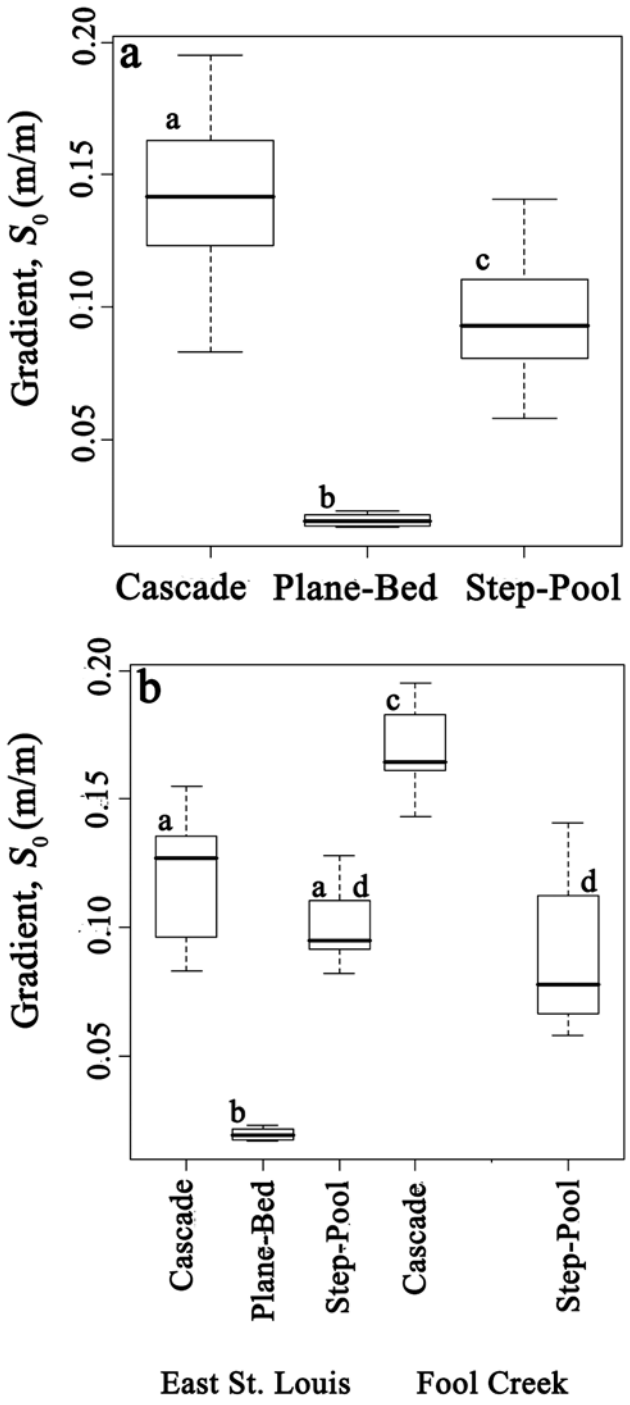

Figure 7. Box plots of (a) gradient versus channel type and (b) gradient versus channel type and basin. The letters a, b, c, and d over each box plot show the results of the Tukey's test following an ANOVA. Box plots with the same letter do not have significantly different means ($p > 0.05$); box plots with different letters do have significantly different means ($p < 0.05$).

the channel types are differentiated by basin, the mean S_0 values between the step-pool and cascade reaches in East St. Louis are not significantly different. Model 11 shows that, holding S_0 constant, there is no consistent difference in $(8/f)^{0.5}$ between cascade and step-pool channels (Table 3). The lack of relationship in model 11 may reflect the large at-a-site variability in these reaches (Figure 6) that is accounted for when flow period or q^* is held constant (model 3 and model 5a). The results therefore do not support the third hypothesis that while holding S_0 constant there is a consistent difference in $(8/f)^{0.5}$ between cascade and step-pool channels.

4.5. Friction Factor, Relative Grain Submergence, and Channel Type (H4)

[38] R_h/D_{84} was found to be significantly related to $(8/f)^{0.5}$. Table 3 shows the regression of R_h/D_{84} and channel type on $(8/f)^{0.5}$ in model 12. The channel type is not significantly related to $(8/f)^{0.5}$ when R_h/D_{84} is held constant. The interaction terms were not tested because there was no significant relationship between $(8/f)^{0.5}$ and channel type. Figure 8a indicates that there are significant differences in R_h/D_{84} between cascade and plane-bed and between step-pool and plane-bed reaches. The variation in $(8/f)^{0.5}$ between plane-bed and other channel types may be better explained by R_h/D_{84} but cannot be further explored because there is only one plane-bed reach. Figure 8b indicates that the difference in standard deviation between cascade and step-pool channels is greater in Fool Creek than in East St. Louis.

[39] R_h/D_{84} is plotted against $(8/f)^{0.5}$ for cascade and step-pool reaches in Figure 9a. The scatter in $(8/f)^{0.5}$ is much broader for the step-pool than for the cascade reaches. A regression using only the cascade reaches (Figure 9b) indicates that there is a significant power relationship between R_h/D_{84} and $(8/f)^{0.5}$. Therefore, holding R_h/D_{84} constant, there is no consistent difference in f between channel types, but a regression restricted to only cascade reaches indicates that a high proportion of the variability in $(8/f)^{0.5}$ is explained by R_h/D_{84} in that channel type. The results thus do not support the fourth hypothesis, that for a given R_h/D_{84} there is a consistent difference in $(8/f)^{0.5}$ between step-pool and cascade reaches. Instead, the significant relationship is between R_h/D_{84} and $(8/f)^{0.5}$ for cascade reaches.

4.6. Friction Factor, Relative Grain Submergence, Wood Load, Gradient, and Dimensionless Unit Discharge for Each Channel Type (H5)

[40] The final hypothesis examines how the significance of the relation of each of these control variables and $(8/f)^{0.5}$ may vary depending on the channel type. Table 4 shows three multiple regressions using only the cascade reaches and four multiple regressions using only the step-pool reaches. The results reemphasize that model 13 only using the cascade reaches with both S_0 and R_h/D_{84} is much better than model 16 which only uses step-pool reaches. The highest proportion of the variability is explained in both channel types when q^* is included in the regression (model 14 and model 19). The regression with the step-pool reaches is greatly improved (adjusted $R^2 = 0.68$) when the variable of relative step submergence (R_h/H) is included, but no relationship was found by including $(H/L_s)/S_0$ (model 18). Including wood load improved both the cascade model (model 15) and the step-pool model (model 18).

[41] Table 4 also shows that the rate of change of q^* with f is different for the two channel types. Both q^* and S_0 have exponents close to −1.0 and 1.0 for the cascade reaches, whereas the exponents for q^* and S_0 is equal to −0.59 and

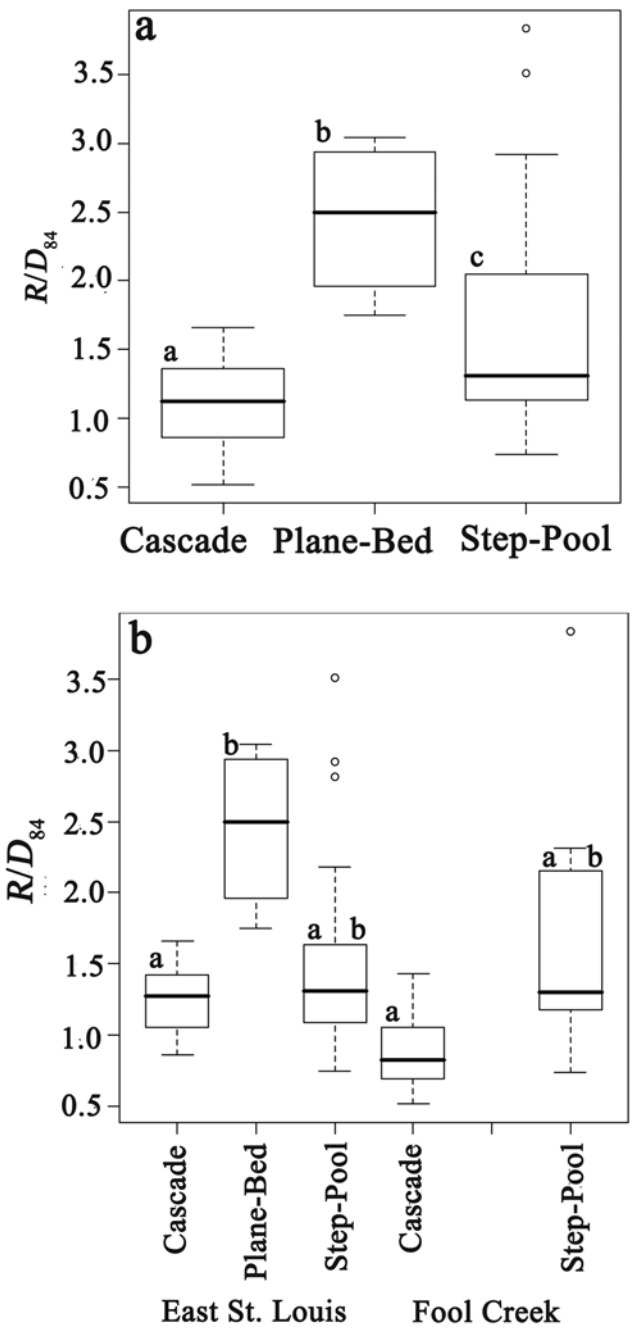

Figure 8. Box plots of (a) relative grain submergence (R/D_{84}) versus channel type and (b) relative grain submergence versus channel type and basin. The letters a, b, and c over each box plot show the results of the Tukey method following an ANOVA. Box plots with the same letter do not have significantly different means; box plots with different letters do have significantly different means ($p < 0.05$).

1.40, respectively, for step-pool reaches. Most likely these differences were not apparent when the interaction terms were tested in Table 3 because the larger variability in the step-pool reaches may have made it difficult to examine the relationships with the cascade reaches. These results support H5, that the components of resistance are sufficiently different in each channel type to change the relationship of the control variables with f in each channel type. This suggests that different control variables should be used when considering the different channel types.

5. Discussion

5.1. Gradient, Dimensionless Unit Discharge, Flow Period, Wood Load, and Friction Factor

[42] Gradient explains a significant proportion of the variability in $(8/f)^{0.5}$ through the channel network, particularly when used in conjunction with the categorical variable of flow period. The relationship shows that f is higher at higher S_0 (Figure 4). The higher the S_0, the more energy is

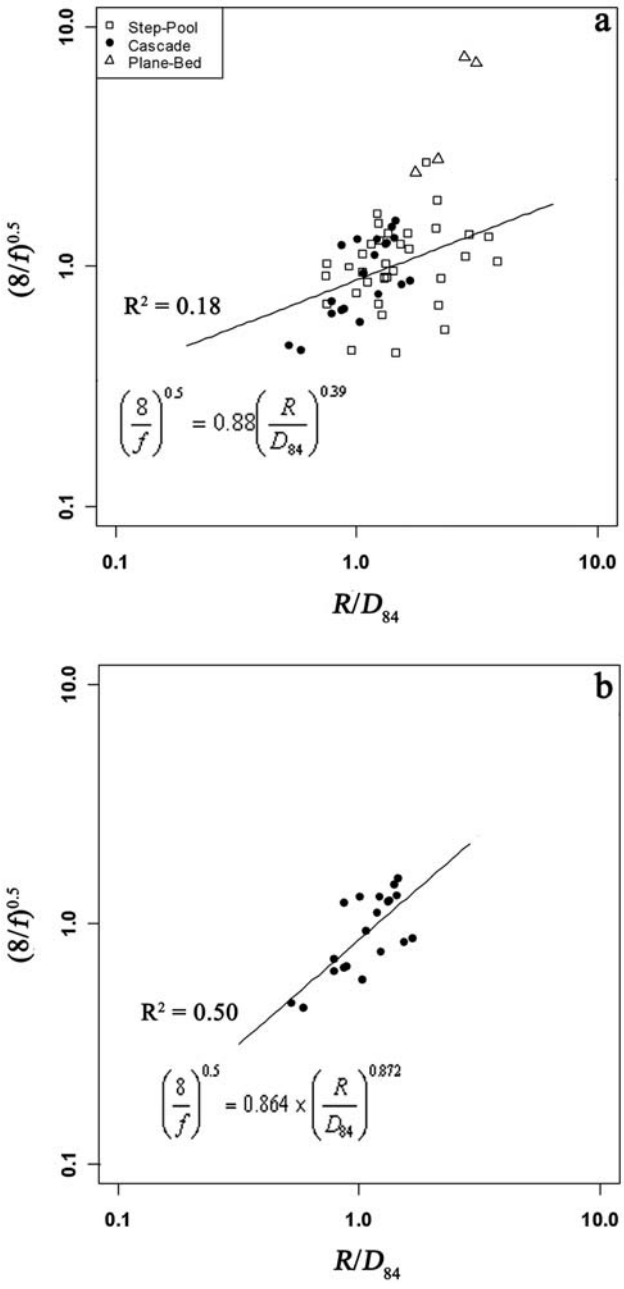

Figure 9. (a) Relative grain submergence versus $(8/f)^{0.5}$ for each channel type. Trendline shows relationship between relative submergence and friction factor for all sites (excluding ESL6, the plane-bed reach). (b) Relative grain submergence versus friction factor for cascade reaches.

Table 4. Linear Regressions of $(8/f)^{0.5}$ and f Versus Independent Variables Separated by Channel Type[a]

	Independent Variables[b]	Cascade Model 13	Cascade Model 14	Cascade Model 15	Step-Pool Model 16	Step-Pool Model 17	Step-Pool Model 18	Step-Pool Model 19
Dependent variables[c]								
$(8/f)^{0.5}$	intercept[d]	0.32*			0.17*			
f	intercept		40.53*	162.06*		6.20*	39.33*	156.00 *
	S_0	−0.50*	1.04*		−0.53*	0.57*		1.40*
	R/D_{84}	0.78*			0.42*			
	q*		−0.90*	−1.10*			−0.73*	−0.59*
	R/H[c]					−1.75*		
	wood load			0.25*	−0.09*		0.15*	
	$(H/L)/S$						0.38	
F statistic		13.62	41.31	19.81	6.57	36.37	11.98	35.74
***p*-value**		<0.001	<0.001	<0.001	0.001	<0.001	<0.001	<0.001
R^2		0.62	0.83	0.70	0.39	0.69	0.55	0.71
Adjusted R^2		0.57	0.81	0.66	0.32	0.68	0.51	0.69

[a]Models 13–15 only include cascade reaches. Models 16–19 only include step-pool reaches.
[b]Variables with asterisks indicate that value is significant at the $\alpha = 0.05$ level.
[c]Variables in bold were transformed using the natural log.
[d]Numbers shown are exponents of independent variables, if it is a categorical variable and that category is true than the number should be multiplied with the intercept.
[e]R_h/H is equivalent to the relative submergence of the step height where H is equal to the average step height from the lowest point in the pool to the top of the step.

likely dissipated from cascading flow and abrupt transitions from supercritical to subcritical. Therefore, S_0 is a significant explanatory variable that is greatly improved when paired with flow period, q*, or wood load (models 1, 5a, and 11).

[43] Many studies have recognized the important correlation between S_0, grain size, step steepness, and channel type [*Bathurst*, 1993; *Abrahams et al.*, 1995; *Montgomery and Buffington*, 1997; *Zimmermann and Church*, 2001; *Wohl et al.*, 2004; *Wohl and Merritt*, 2005; *Wohl and Merritt*, 2008], and our results plus some additional analysis indicate that bed gradient is related to each of these variables (Figure 7). Conversely, a significant difference in f was not found to exist between step-pool and cascade channels for a given S_0 (model 11). The channel types represent the bed morphology and the potential variability in flow resistance from either spill resistance in step-pool channels to grain resistance in cascade reaches, with form resistance being prominent in both [*Curran and Wohl*, 2003; *Wilcox et al.*, 2006; *Comiti et al.*, 2007]. Both models 11 and 12 show that $(8/f)^{0.5}$ is not significantly different for step-pool and cascade reaches. Therefore, the type of resistance (i.e., grain, form, or spill) may vary based on channel type, but the total flow resistance is similar for both.

[44] The effect of bed gradient is likely related to its relationship to other explanatory variables such as D_{84}, H/L_s, and the Froude number (Fr) [*Abrahams et al.*, 1995; *Church and Zimmermann*, 2007; *Comiti et al.*, 2009]. All of these variables are highly interrelated. At higher slopes, the flow depth is shallower and the boulders larger in relation to the flow depth. An object that protrudes through the surface creates greater surface drag, which varies with Fr [*Bathurst*, 1982]. The Fr is highly variable throughout the reach as localized areas of supercritical flow and hydraulic jumps develop. There is greater energy dissipation and turbulence at low flows as flow separates around individual boulders [*Wohl and Thompson*, 2000]. As flow increase, these larger elements may become quickly submerged creating localized skimming flows, where water flow becomes more planer between successive objects [*Chanson*, 1994]. The larger change in depth between low and high flows at steeper gradients may cause a much larger reduction in the total flow resistance, in comparison with the lower gradient reaches, as boulders are quickly submerged [*Pagliara and Chiavaccini*, 2006]. Also, as flow increases the number of particles that influence the surface are reduced as smaller cobbles and boulders are submerged (Figure 10).

[45] Flow period, q*, and other relative submergence variables (R/D_{84}, R_h/H, R/s_{bed}) were all significant explanatory variables and represent the influence of discharge on total f (Tables 3 and 4). As discharge increases in each channel type, the flow patterns vary and total f decreases. The drop from the step lip to the pool is larger at low flows; therefore, more energy is lost from larger steps and spill resistance dominates [*Comiti et al.*, 2009]. Conversely, at high flows there are larger hydraulic jumps and more turbulence through the velocity profile [*Wilcox and Wohl*, 2007], which dissipates a large amount of energy. *Comiti et al.* [2009] identified nappe and skimming flow regimes as two distinct regimes in step-pool channels. Additionally, *Comiti et al.* [2009] found that the type of resistance that dominates in step-pool reaches (i.e., grain, form, or spill) depend on the flow regime. In step-pool reaches, flow transitions from nappe flow at low discharges to skimming and submerged at the highest flows [*Church and Zimmermann*, 2007; *Comiti et al.*, 2009]. Nappe flow is free-falling flow over steps into a pool [*Chanson*, 1994]. Skimming flow is where flow becomes more planar over the step and air pockets disappear. Flow in this regime becomes supercritical [*Comiti et al.*, 2009]. Submerged flow occurs when flow over the step is affected by the downstream tailwater [*Church and Zimmermann*, 2007]. Nappe flow existed in a majority of the steps in the current research over all flow periods. Skimming flow was observed over a limited number of steps during June 2008 flows, particularly over the boulder steps at lower S_0. Submerged flow was only observed over the smaller steps identified in FC1. An added component

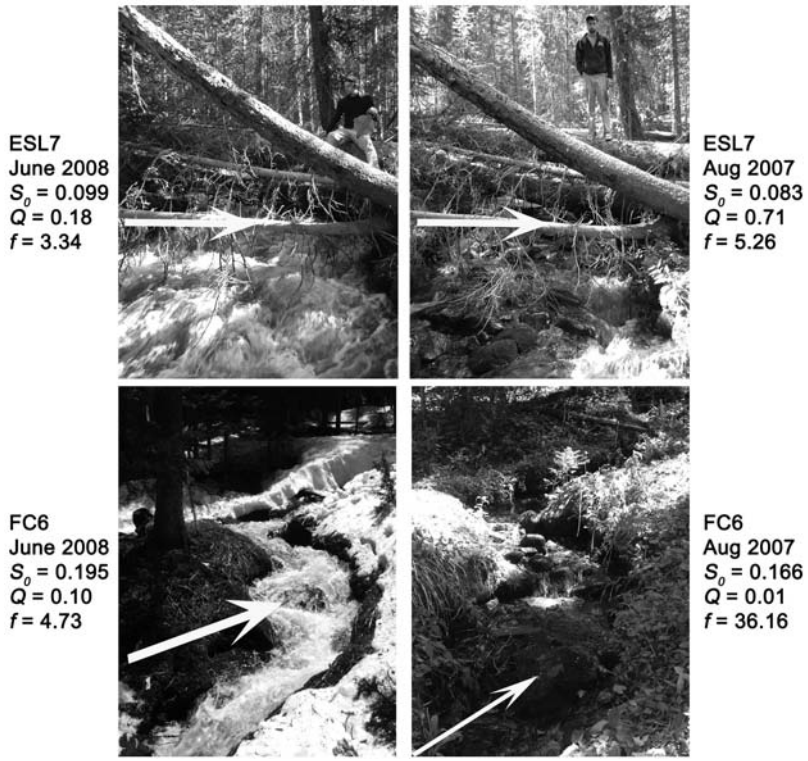

Figure 10. Two cascade reaches at low (August 2007) and high (June 2008) flows. Arrows point to the same location on both images. Images show that at high flow the majority of grains are submerged in FC6 while in ESL7 the location of the grains is still visible.

in many of these reaches is flow over and through the porous wood steps versus flow over large boulder steps. When flow drops over wood steps at low flows, the drop is higher and the jet does not plunge immediately from the step lip to the pool. At higher flows the water more easily flows from the step lip to the pool. Once skimming flow occurs, form and grain resistance increase as spill resistance decreases with the drop height. Form resistance increases as the water surface gradient steepens in the pools [*Comiti et al.*, 2009]. The large variability in step type and flow regime over the step-pool reaches explains the greater variability in $(8/f)^{0.5}$ over all flow periods and reaches (Figure 9).

[46] In cascade reaches at lower flows, larger grains protrude through the surface, creating wave drag and increasing the total f in a reach [*Smart et al.*, 2002]. One or two steps and pools exist in some of the cascade reaches, but the variability in these reaches is not as large as in the step-pool reaches (Figure 9); therefore, the total resistance in cascade reaches is more easily explained by a small number of control variables (Table 4; models 13 to 15). Overall, the results of the regressions show that the total f is highest at low flows and lowest at high flows for all the reaches, indicating that individual grains and bed forms more effectively retard the flow at lower discharges.

[47] Dimensionless unit discharge, q^*, provides another way to represent relative grain submergence and differences in flow. The reason for the improved relationship between q^* and f versus the R_h/D_{84} is not completely understood. *Ferguson* [2007] proposed that there is a reduction in measurement error when q^* is used, rather than R_h/D_{84}, because any error in D_{84}, Q or V affects both the observed and predicted values of velocity. Alternatively, any error in R_h/D_{84} will affect either predicted or observed velocities but not both at the same time. It is also possible that in using q^*, the inclusion of width ($q = Q/W$) in the relative submergence variable improves its explanatory power. Therefore, q^* was found to be an improved metric for representing both flow and relative submergence in these steep gradient streams, but more work needs to be done to understand why it explains so much more variability than R_h/D_{84}.

[48] The differences in the ability of individual control variables (S_0, R_h/D_{84}, and q^*) to explain the variability in $(8/f)^{0.5}$ is demonstrated in Figure 11. Figures 11a and 11b show that the error in predicting f by using S_0 and R_h/D_{84} is greatest at the lowest flows, which correlates to the highest values of $(8/f)^{0.5}$ (FC1 and FC2). Figure 11c shows that a model with q^* (model 9; Table 3) greatly improves the prediction of $(8/f)^{0.5}$, but the FC1 and FC2 are still underpredicted. Figure 11d shows the prediction of a combined multiple regression (model 5a; Table 3) which includes q^*, S_0, and channel type. The inclusion of S_0 and channel type greatly improves the overall error, but values of $(8/f)^{0.5}$ are overpredicted for step-pool reaches and underpredicted for cascade reaches. The highest error in Figure 11d is in the prediction of $(8/f)^{0.5}$ for ESL2 and FC3, which were often distinguished as outliers.

[49] Although these regressions are meant for explanatory purposes and not for prediction, Figure 11, Table 3, and Table 4 help to demonstrate which variables may be useful for developing new predictive equations in these higher-gradient streams. Inclusion of a flow variable (q^*), gradient and channel type increase the ability to explain the variability in FC1 and FC2 (Figure 11d) but do not explain the

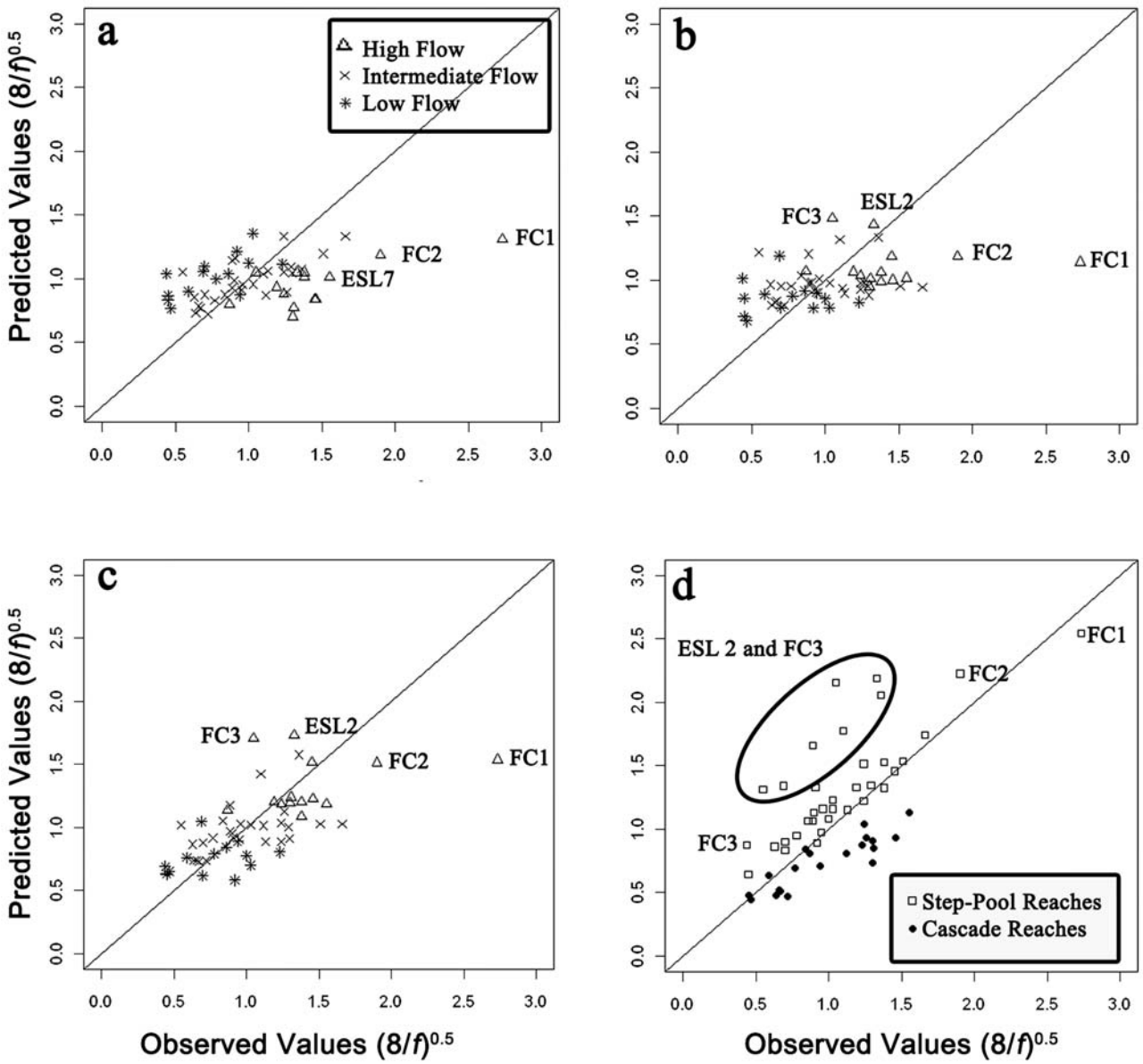

Figure 11. Predicted versus observed $(8/f)^{0.5}$ for (a) model 7 (S_0), (b) model 8 (R/D_{84}), (c) model 9 (q^*), (d) model 5a (q^*, S_0 and channel type).

variability as well in ESL2 and FC3. FC1 and FC2 have some of the smallest grain sizes, smallest amounts of wood and lowest S_0 (Table 2). FC1 may even be a transition reach between a plane-bed and step-pool. The values of total flow resistance in both reaches are the lowest (Table 2), except for the plane-bed reach (ESL6). In model 5a, S_0 is a proxy for both grain size and step steepness, which combines with q^* and channel type to better explain the variability in these two reaches. On the other hand, S_0, q^*, and channel type cannot account for the higher values of total flow resistance in ESL2 and FC3 because wood load dominates in these reaches, meaning that form drag and spill resistance dominate and including only a grain submergence variable (q^*) does not help explain the greater variability.

[50] Wood load was found to be significantly related to total f for all reaches (Table 3) and for regressions evaluating only step-pool or cascade reaches (Table 4). The importance of wood in step-pool channels have been noted by other researchers in both flume studies [*Wilcox et al.*, 2006] and field studies [*Curran and Wohl*, 2003; *Manners et al.*, 2007; *Comiti et al.*, 2008]. *Wilcox et al.* [2006] found that wood located at the step lip contributed both to the structure of the step and increased the step height, which subsequently increased the spill resistance. Both *Manga and Kirchner* [2000] and *Hygelund and Manga* [2003] determined that the presence of wood increases the depth of flow in a channel, increasing the total shear stress, but that the shear stress acting on the bed decreases as wood density increases. The wood increases the resistance, decreasing the total shear stress available for bed or bank erosion and sediment transport is reduced. *Curran and Wohl* [2003] also concluded that step-forming wood contributes more to total flow resistance than wood found as individual pieces throughout the reach. *Wilcox et al.* [2006] showed that grain roughness was greatly reduced once steps or wood were present. The flume study done by *Wilcox et al.* [2006] did

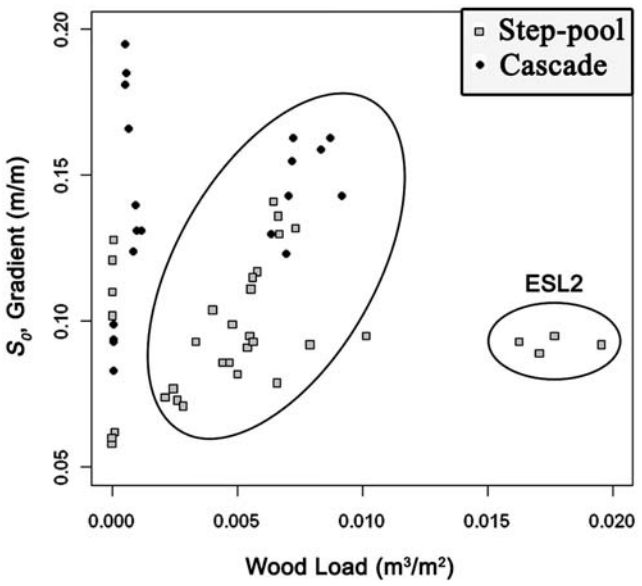

Figure 12. Wood load versus S_0 for step-pool and cascade channel types. Reaches in oval are linearly correlated with S_0 except for ESL2.

not include the boulder steps found in reaches in the current study and the more heterogeneous grain size distribution. Variables related to both grain roughness (R/D_{84} and q^*) and wood were both significant explanatory variables (Table 3; models 4b and 5b). The majority of the wood is found in steps; therefore, the significance of wood load on f is related to the significance of steps. The greater heterogeneity in grain size and step types (boulder and wood) probably accounts for the greater significance of variables related to grain roughness. S_0 is a significant explanatory variable in all regressions and is another variable that is correlated with both grain size and is slightly correlated with wood (Figure 12). For all reaches, except for ESL2, that has a significant amount of wood, wood load increases with S_0. Most likely, this is related to an increase in step steepness as log steps increase step height, therefore creating steeper gradients [*Comiti et al.*, 2008]. The positive correlation between S_0 and wood load is even greater in the channel type regressions (Table 4); thereforev S_0 is left out of regressions that include wood load. Wood load is positively related with f and is a better explanatory variable in cascade reaches versus step-pool reaches. The cascade reaches have higher variability in the amount of wood in each reach and where the wood is located, which may account for the better relationship between the wood load and f. The step-pool reaches all have a large amount of wood, except for ESL4 and FC1, and most of that wood is found in the steps. The wood load in these reaches mainly represents the size of the steps, which is better represented by R_h/H.

[51] There was not a significant difference in the variability in f between channel types holding S_0 constant (model 11), signifying that grain, form, and spill resistance may vary based on the channel type, but that total f varies in predictable ways with S_0 and flow, despite the differences between step-pool and cascade reaches. The differences between individual reaches may be more significant than the differences between channel types. Also, channel type was found to only be significant in regression models that included S_0 and did not include wood, suggesting that channel type cannot be used as a proxy for S_0. Gradient, R_h/D_{84}, and f overlap for the cascade and step-pool reaches because some of these reaches overlap in characteristics. Some of the cascade reaches have steps and pools, which may indicate that these reaches are transitional between step-pool and cascades rather than distinct cascading reaches. Despite similarities, Table 4 indicates that different control variables explain a greater proportion of the variability in step-pool versus cascade reaches.

5.2. Relative Grain Submergence, Dimensionless Unit Discharge, Standard Deviation of Bed Elevation, Relative Step Submergence, and Darcy-Weisbach Friction Factor

[52] Relative grain submergence is a measure that is commonly equated with grain resistance in a channel [*Wilcox et al.*, 2006]. We found that R_h/D_{84} correlated positively with $(8/f)^{0.5}$, meaning that at high values of R_h/D_{84}, f is at its lowest value in the channel. There is significant correlation between these variables, but the low adjusted R^2 (0.16) indicate that the proportion of variability explained by the relationship is minimal. The use of R_h/D_{84} in equations to estimate both the friction and velocity in a stream is based on turbulent boundary layer theory, where the flow is affected by the friction at the boundary of the channel and varies with distance from the boundary [*Bathurst*, 1993]. Many relations were developed that equate R_h/D_{84} to f for lower gradient channels using either the logarithmic law of the wall or an empirical power law equation [*Keulegan*, 1938; *Bathurst*, 1993, 2002; *Katul et al.*, 2002]. *Comiti et al.* [2007], along with others [*Wiberg and Smith*, 1991; *Ferguson*, 2007], also found that for large-scale roughness, which was defined as $R_h/D_{84} < 1.8$, resistance equations based on the approach of the law of the wall may be invalid. Most of the reaches in this study remain within the range of large-scale roughness; therefore, the use of R_h/D_{84} may be inappropriate for these reaches.

[53] *Lee and Ferguson* [2002] concluded that a power law gives the best fit when the roughness height, k_s, is estimated by the step D_{50} rather than a reach-averaged grain size. The use of a reach-averaged grain size in this paper may be another explanation for the poor correlation between R_h/D_{84} and f, particularly in the step-pool reaches (Table 4). *Baiamonte and Ferro* [1997] showed that a scale parameter, size distribution parameter, and particle arrangement parameter should be used together to more appropriately account for coarser bed elements. More work needs to be done to determine if any of these parameters would be appropriate for representing grain resistance in these reaches.

[54] The relationship between $(8/f)^{0.5}$ and R_h/D_{84} has a lot of scatter at all flows, but the largest error is in the prediction of $(8/f)^{0.5}$ for FC1 and FC2 at the August 2007 low flow (Figure 11b). *Ferguson* [2007] showed that equations split between shallow flows and deep flows were the best predictors of velocity, although all submergence-based equations had a high error in predicting the velocity, particularly at lower flows ($R_h/D_{84} < 1$). *Bathurst* [2002] found that the relationship between $(8/f)^{0.5}$ and R_h/D_{84} changed with S_0. Model 4a (Table 3) shows that including both R_h/D_{84} and S_0 together improves the regression, but the low adjusted R^2

indicate that other combination of variables are needed to explain a greater proportion of the variability in $(8/f)^{0.5}$.

[55] A model with R_h/D_{84} is greatly improved by including wood load (model 4b) instead of channel type, suggesting that wood load is a better predictor than channel type (model 4a). Wood is related to both form drag around individual pieces and spill resistance over steps [*Curran and Wohl*, 2003]. The majority of the wood found in both channel types is located in the steps, creating an interrelationship between wood load and bed morphology. There is also a slight positive relationship between wood load and S_0 (Figure 12), which is described in section 5.1. Model 4a indicates that R_h/D_{84} is a poor surrogate for flow (Figure 11b), but inclusion of a wood parameter accounts for a much larger proportion of the variability in total flow resistance. *Buffington and Montgomery* [1999] found that pool riffle and plane-bed reaches with increased wood, caused increased hydraulic roughness and textural fining of the particle size distribution. In the current study, no significant relationship was found between wood load and D_{84}, although the reaches with the largest wood loads, ESL2 and FC3, have the smallest particle size in both basins. The interrelationship between wood load, particle size, and S_0 may account for the difficulty in describing the variability in ESL2 and FC3. Localized fining was also noted behind some of the larger wood steps in ESL1, ESL8, ESL9, and FC4, but these localized areas were not large enough to noticeably influence the reach-averaged values. The same effect of localized fining was not observed upstream of boulder steps. The wood load represents both form and spill resistance and together with R_h/D_{84} the grain resistance is encompassed in the multiple regression.

[56] *Comiti et al.* [2007], *Aberle and Smart* [2003], and *Rickenmann* [1991] proposed using dimensionless unit discharge (q^*) in place of R_h/D_{84} for steep gradient streams. This approach was initially developed to relate q^* with a dimensionless velocity ($v^* = V/(gD_{84})^{0.5}$), but here as well as by *Comiti et al.* [2007] it is used to understand the variability in f. Model 9 (Table 3) demonstrates that this parameter explains a greater proportion of the variability in f than either R_h/D_{84} or S_0. *Ferguson* [2007] also found that q^* has the lowest error for predicting velocity in a reach. Figures 11c and 11d demonstrate that including q^* has a similar effect in predicting f as including a categorical variable for flow period; therefore, q^* is effectively representing the changes in roughness that occur as flow increases. Unfortunately, this parameter is only useful if the Q is already known and V is being predicted. If both Q and V need to be predicted, some other measure of the effect of flow variation should be considered.

[57] Another measure of bed roughness, R_h/s_{bed}, was proposed by *Aberle and Smart* [2003] to be a more appropriate measure of the roughness structure in a steep gradient channel than the grain size. *Aberle and Smart* [2003] argued that beds armored with the same mean grain diameter may have a completely different roughness structure. *Baiamonte and Ferro* [1997] also showed the importance of the spatial arrangement of particles. Therefore, the s_{bed} is used as a measure of the roughness structure. We used a similar methodology as *Comiti et al.* [2007] by regressing the two grain size parameters (D_{84}, D_{50}) and s_{bed} against velocity to determine which variable explains a greater proportion of the variability in velocity. These roughness parameters are all on the same order of magnitude as the water depth; therefore, each is expected to have some relationship with f. The most significant relationship was between D_{84} and velocity. There was no significant relationship between s_{bed} and velocity, although R_h/s_{bed} was found to be a better measure for predicting flow resistance than R_h/D_{84} or q^* (Table 3; models 4a, 6, and 9). Some spurious correlation exist between R_h and f, since R_h is used in the calculation of f, but that does not account for the high adj-R^2 when relating R_h/s_{bed} to f. Although, R_h/s_{bed} is a significant variable and may be a preferred variable for developing an equation to predict f, the physical significance of this relationship is unclear since s_{bed} was not found to be related to V. The lack of correlation between s_{bed} and V may be because the measurement spacing was not narrow enough (~15 to 20 cm). Also, s_{bed} represents the standard deviation of the bed elevation along the thalweg and not over the entire bed. *Church and Zimmermann* [2007] suggest that the s_{bed} does not adequately describe how velocity may vary over a step-pool reach during lower flows. The poor correlation between s_{bed} and f agrees with *Comiti et al.*'s [2007] analysis of high-gradient channels.

[58] The multiple regressions in Table 4 indicate that a greater proportion of the variability can be explained by including relative step submergence (R_h/H) in step-pool reaches and relative grain submergence (R_h/D_{84}) in cascade reaches if q^* cannot be used. These results suggest that despite similarities in f and even S_0, the types of resistance (i.e., grain, form, or spill) are sufficiently different in these two channel types that other control variables should be considered when attempting to predict V. *Comiti et al.* [2009] found in a flume study of step-pool channels that in order to predict total flow resistance, there must be some differentiation between low and high flows or, in the step-pool reaches, between nappe and skimming flows. The results of the regression analysis in the present study support that conclusion (Table 3). R_h/H can be a measure of flow regime as steps become more submerged the flow will move from nappe to skimming flow. Wood load is not used in a model with R_h/H because the two variables are interrelated since wood load is related to step height.

[59] *Jarrett* [1984] found that S_0 is a better parameter than R_h/D_{84} for predicting f in high-gradient channels. The results of the present study indicate that both relationships are significant, but neither works better than the other, although a more appropriate flow parameter (q^*, flow period) and wood load can be coupled with S_0 for an improved model.

5.3. Channel Type and Friction Factor

[60] A significant difference in total f exists between the plane-bed reach and both step-pool and cascade channel types (Figure 5). Only one plane-bed reach is used in this study and although it is significantly different from the two other channel types, more work needs to be done to determine if this reach appropriately represents all plane-bed reaches. The step-pool and cascade reaches were not found to have significantly different means. The step-pool and cascade channel types were only found to be significantly different while holding both S_0 constant together with a flow variable (Table 3). Although cascade and step-pool channel types may vary in terms of S_0 and D_{84}, the values of total f are high for both of these channel types in these high-gra-

dient streams. The greatest variability between channel types is the type of flow resistance that dominates and therefore the parameters that best explains the variability in f differ. R_h/D_{84} better explains the variability in f in cascade reaches versus step-pool reaches (Figure 9 and Table 4). Many other researchers have noted the lack of correlation between R_h/D_{84} and f in step-pool streams [*Aberle and Smart*, 2003; *Church and Zimmermann*, 2007; *Comiti et al.*, 2007; *Wohl and Merritt*, 2008]. The correlation between R_h/D_{84} and f in the cascade reaches may indicate that grain roughness dominates in these reaches, leading to the closer correlation with a variable that includes the grain size. Wood load is also a significant source of variability in these cascade reaches and together with another grain submergence variable, q^*, explains the largest proportion of variability (Table 4; model 15). Model 15 shows that for a given q^*, wood load increases with f. Therefore, form resistance is still a significant source of resistance in these cascade reaches.

[61] Form and spill resistance most likely dominate in the step-pool reaches [*Curran and Wohl*, 2003; *Church and Zimmermann*, 2007; *Ferguson*, 2007; *Comiti et al.*, 2009]; therefore, R_h/D_{84} is not appropriate for describing the variability in f in this channel type. Despite the dominance of form and spill resistance, a different form of grain roughness, q^*, does work for step-pool reaches (model 19). The models that explain the greatest proportion of variability in f in step-pool reaches are the ones with either R_h/H or q^* (Table 4; models 17 and 19). R_h/H represents spill resistance over steps by representing the height that the water falls over each step. Larger values of R_h/H mean that steps are becoming more submerged and the drop from the step lip to the pool is reduced, causing a reduction in the contribution of spill resistance to total flow resistance [*Comiti et al.*, 2009]. Skimming flow occurred over a proportion of the steps in each reach during high flows, causing a reduction in spill resistance from these steps. Form and grain resistance would then begin to dominate at higher flows [*Comiti et al.*, 2009]. Wood load does not greatly improve the explanatory power of any of the step-pool models (Table 4; models 16 and 18). The high correlation between wood load and S_0 in step-pool reaches mean that when S_0 is included in a regression, it also represents wood load. Therefore, the regressions with S_0 and R_h/H or q^* better explain the variability in step-pool reaches than the regressions that include wood load (Table 4).

[62] The step steepness (H/L_s) is positively related to S_0 through a power function, meaning that as S_0 increases the H increases in relation to L_s. H/L_s represent the three distinct sections that make up a step-pool channel, where velocity varies from critical to supercritical to subcritical: the step lip, the pool, and the run. Flow over the step lip is critical right before the water plunges into the pool. In the pool, there is a sharp velocity reduction as water goes from supercritical to subcritical [*Leopold et al.*, 1964]. Therefore, pools are dominated by hydraulic jumps and wake turbulence [*Wohl and Thompson*, 2000; *Church and Zimmermann*, 2007]. The greatest amount of energy is dissipated as flow plunges over the steps and decelerates in the pools [*Wohl and Thompson*, 2000]. The runs, also known as the step treads, are the areas just upstream of the pool. Flow accelerates through the runs and just as it plunges over the step lips, reducing turbulence in these sections. *Wohl and Thompson* [2000] concluded that the higher average velocities in the runs means that grain resistance is not as effective an energy dissipater as form drag around the steps and wake generated turbulence in the pools. The relationship between S_0 and H/L_s mean that at higher gradients there are steeper steps with shorter runs and thus a higher elevation difference between the step lip and the pool. Therefore, more energy may be dissipated by the steps at these higher gradients. In model 18 the steepness factor $(H/L_s)/S$ was not found to be significantly related to f in step-pool reaches, but wood load, R_h/H, and S_0 were significant and are related to step geometry. No significant relationship was found between f and individual step geometry variables (H, L_s, and H/L_s). These results support *Curran and Wohl*'s [2003] conclusion that step geometry may not be an appropriate measure for estimation f. Conversely, R_h/H is significant in step-pool reaches, despite the lack of significance of H and, just like R_h/s_{bed}, may still be an important variable when considering developing a predictive equation in high-gradient channels. Furthermore, the regression results support the idea that each of these control variables represents a different form of resistance in these reaches. Therefore, if Q is unknown, then the f and subsequently V can be better approximated by R_h/D_{84} in cascade reaches and R_h/H in step-pool reaches.

5.4. Other Sources of Variability

[63] *Bathurst* [1985] noted that at-a-site variability in f was much greater than between-site variability for his data. Figure 6 shows the large differences in at-a-site and between-site variability in $(8/f)^{0.5}$ for each channel type and in each drainage basin. There are many other sources of variability in these channels that are not accounted for with these simple parameters tested in the above regressions. For instance, expansions and contractions of the channel banks can be an important source of resistance [*Bathurst*, 1985; *Kean and Smith*, 2006]. The purpose of the above analysis were to find simple reach average variables that may eventually be used to develop a predictive equation for high gradient streams, but these other sources of variability will be explored further in subsequent analyses.

6. Conclusion

[64] Past work suggests that gradient and discharge are the dominant controls on f in steep mountain streams. S_0 coupled with one or two other explanatory variables greatly improved the proportion of variability explained in any model. It is important to understand how S_0 is related to f and other stream characteristics, since this is a metric that can be used to remotely predict these characteristics, as the resolution of remote data improves with time [*Wohl et al.*, 2007]. Further work needs to be completed to couple the results of these regressions with development of a predictive equation for high-gradient channels. The regression analysis supports the conclusions of *Comiti et al.* [2009] developed from a flume study on step-pool channels, in that a parameter that represents the flow regime needs to be included for the best predictive models of f. Both q^* and flow period coupled with S_0 had the greatest explanatory power and would most likely have the best predictive capabilities.

[65] The different forms of resistance that dominate in each channel type were mirrored by the different indepen-

Table A1. Average Values for Reach Dimensions and Hydraulic Variables for the Four Flow Periods in Each Reach

Reach	Channel Type	Flow Period	L_r[a] (m)	S_0 (m/m)	A (m^2)	R (m)	W (m)	H (m)	L_s (m)	D_{50} (m)	D_{84} (m)	V (m/s)	Q (m^3/s)	u^* (m/s)	Fr	Re	f
ESL1	step-pool	Jun 2008	29.37	0.093	0.99	0.25	2.92	0.63	4.64	0.05	0.16	0.66	0.66	0.49	0.36	1.5E+05	4.23
		Jul 2008	27.30	0.104	0.70	0.20	2.60	0.76	4.31	0.05	0.16	0.41	0.29	0.46	0.25	7.3E+04	9.81
		Aug 2007	31.57	0.086	0.29	0.12	2.01	0.62	4.97	0.05	0.16	0.22	0.06	0.32	0.19	2.2E+04	16.32
ESL2	step-pool	Jun 2008	13.70	0.093	1.00	0.25	3.21	0.52	2.56	0.01	0.07	0.63	0.63	0.48	0.35	1.4E+05	4.51
		Jul 2008	13.99	0.089	0.74	0.21	2.97	0.44	2.75	0.01	0.07	0.60	0.44	0.45	0.37	1.1E+05	4.35
		Jul 2007	13.95	0.095	0.68	0.20	2.86	0.35	2.58	0.01	0.07	0.46	0.31	0.42	0.29	8.0E+04	6.60
		Aug 2007	14.04	0.092	0.45	0.15	2.57	0.46	2.78	0.01	0.07	0.25	0.11	0.38	0.18	3.4E+04	16.84
ESL3	cascade	Jun 2008	10.24	0.140	0.87	0.18	3.63	0.51	0.77	0.06	0.13	0.73	0.64	0.48	0.48	1.2E+05	3.75
		Jul 2008	10.69	0.124	0.80	0.17	3.54	0.48	1.30	0.06	0.13	0.60	0.48	0.45	0.41	9.1E+04	5.02
		Jul 2007	10.69	0.131	0.61	0.15	3.03	0.48	1.57	0.06	0.13	0.50	0.30	0.43	0.36	6.8E+04	6.34
		Aug 2007	11.32	0.131	0.42	0.14	2.41	0.48	1.03	0.06	0.13	0.39	0.16	0.40	0.29	4.8E+04	9.15
ESL4	step-pool	Jun 2008	15.57	0.128	0.99	0.26	2.86	0.53	2.22	0.07	0.17	0.69	0.68	0.56	0.37	1.6E+05	5.17
		Jul 2008	16.31	0.110	0.78	0.23	2.69	0.60	2.64	0.07	0.17	0.51	0.40	0.51	0.30	1.0E+05	7.56
		Jul 2007	15.75	0.121	0.57	0.18	2.48	0.55	2.87	0.07	0.17	0.45	0.26	0.47	0.30	7.2E+04	8.85
		Aug 2007	16.54	0.102	0.50	0.17	2.32	0.47	2.49	0.07	0.17	0.33	0.16	0.45	0.23	5.0E+04	13.15
ESL5	cascade	Jun 2008	12.50	0.155	1.20	0.24	4.04	1.03	1.00	0.05	0.14	0.52	0.63	0.61	0.30	1.1E+05	10.66
		Jul 2008	13.89	0.130	1.09	0.22	3.95	0.70	3.40	0.05	0.14	0.45	0.49	0.56	0.27	8.8E+04	11.22
		Jul 2007	13.51	0.143	0.78	0.18	3.58	0.87	1.04	0.05	0.14	0.38	0.29	0.51	0.26	5.9E+04	13.46
		Aug 2007	15.11	0.123	0.59	0.15	3.25	0.88	1.18	0.05	0.14	0.25	0.15	0.44	0.19	3.3E+04	22.85
ESL6	plane-bed	Jun 2008	6.40	0.018	0.89	0.26	2.98	N/A	N/A	0.02	0.09	1.67	1.85	0.25	0.97	3.8E+05	0.16
		Jul 2008	6.42	0.020	0.79	0.24	2.85	N/A	N/A	0.02	0.09	1.43	1.13	0.19	0.86	3.0E+05	0.14
		Jul 2007	6.54	0.017	0.56	0.19	2.69	N/A	N/A	0.02	0.09	0.60	0.34	0.17	0.42	9.8E+04	1.02
		Aug 2007	6.22	0.023	0.44	0.15	2.65	N/A	N/A	0.02	0.09	0.42	0.18	0.17	0.33	5.5E+04	1.31
ESL7	cascade	Jun 2008	22.10	0.099	0.97	0.25	3.02	N/A	N/A	0.08	0.17	0.73	0.71	0.46	0.41	1.6E+05	3.34
		Jul 2008	23.99	0.093	0.86	0.23	2.93	N/A	N/A	0.08	0.17	0.54	0.46	0.42	0.32	1.1E+05	5.18
		Jul 2007	22.86	0.094	0.57	0.18	2.71	N/A	N/A	0.08	0.17	0.51	0.29	0.39	0.35	7.9E+04	4.74
		Aug 2007	24.31	0.083	0.42	0.15	2.46	N/A	N/A	0.08	0.17	0.43	0.18	0.35	0.32	5.7E+04	5.26
ESL8	step-pool	Jun 2008	30.68	0.099	0.91	0.23	3.16	0.39	4.50	0.07	0.17	0.62	0.57	0.44	0.37	1.3E+05	4.22
		Jul 2008	32.65	0.086	0.78	0.21	3.03	0.42	4.58	0.07	0.17	0.55	0.43	0.43	0.34	1.0E+05	4.82
		Jul 2007	31.38	0.091	0.59	0.18	2.73	0.41	4.48	0.07	0.17	0.46	0.27	0.40	0.31	7.4E+04	6.22
		Aug 2007	35.48	0.082	0.48	0.16	2.58	0.43	5.87	0.07	0.17	0.36	0.17	0.36	0.26	5.1E+04	8.05
ESL9	step-pool	Jun 2008	16.26	0.115	0.92	0.25	2.79	0.44	2.62	0.06	0.15	0.62	0.57	0.49	0.34	1.4E+05	5.60
		Jul 2008	16.51	0.111	0.72	0.22	2.62	0.43	2.69	0.06	0.15	0.46	0.33	0.45	0.28	8.7E+04	8.68
		Jul 2007	16.22	0.117	0.64	0.20	2.53	0.46	2.59	0.06	0.15	0.42	0.27	0.45	0.27	7.3E+04	10.00
		Aug 2007	18.64	0.095	0.47	0.17	2.28	0.44	3.08	0.06	0.15	0.34	0.16	0.39	0.24	5.0E+04	10.78
FC1	step-pool	Jun 2008	23.12	0.062	0.38	0.16	1.97	0.20	2.78	0.03	0.08	0.86	0.33	0.32	0.63	1.2E+05	1.07
		Jul 2008	23.20	0.060	0.17	0.10	1.57	0.20	3.22	0.03	0.08	0.29	0.05	0.24	0.29	2.5E+04	5.18
		Jul 2007	23.74	0.060	0.18	0.10	1.63	0.19	2.83	0.03	0.08	0.41	0.08	0.25	0.39	3.6E+04	2.90
		Aug 2007	25.12	0.058	0.09	0.06	1.28	0.19	2.42	0.03	0.08	0.20	0.02	0.19	0.24	1.1E+04	7.58
FC2	step-pool	Jun 2008	14.38	0.074	0.39	0.18	1.63	0.25	2.30	0.03	0.08	0.68	0.26	0.35	0.44	1.0E+05	2.23
		Jul 2008	14.18	0.077	0.20	0.11	1.41	0.22	2.44	0.03	0.08	0.25	0.05	0.28	0.22	2.4E+04	9.59
		Jul 2007	15.05	0.073	0.17	0.10	1.41	0.19	3.01	0.03	0.08	0.41	0.07	0.27	0.37	3.6E+04	3.49
		Aug 2007	14.93	0.071	0.08	0.06	1.13	0.20	2.72	0.03	0.08	0.19	0.01	0.20	0.23	1.0E+04	9.39
FC3	step-pool	Jun 2008	13.48	0.093	0.55	0.19	2.12	0.36	2.51	0.01	0.05	0.43	0.24	0.42	0.27	7.2E+04	7.24
		Jul 2008	12.22	0.092	0.24	0.11	1.66	0.29	2.44	0.01	0.05	0.18	0.04	0.33	0.15	1.8E+04	26.92
		Jul 2007	14.87	0.079	0.23	0.11	1.64	0.33	3.55	0.01	0.05	0.27	0.06	0.31	0.23	2.6E+04	10.04
		Aug 2007	11.90	0.095	0.12	0.07	1.36	0.32	2.92	0.01	0.05	0.11	0.01	0.28	0.12	6.9E+03	42.13
FC4	step-pool	Jun 2008	18.86	0.141	0.49	0.20	1.65	0.49	2.87	0.05	0.10	0.75	0.37	0.52	0.44	1.3E+05	3.82
		Jul 2008	19.82	0.130	0.21	0.12	1.39	0.42	3.63	0.05	0.10	0.27	0.06	0.38	0.22	2.8E+04	16.20
		Jul 2007	19.01	0.136	0.23	0.12	1.45	0.49	2.97	0.05	0.10	0.25	0.06	0.40	0.20	2.7E+04	19.90
		Aug 2007	19.23	0.132	0.14	0.09	1.25	0.38	3.01	0.05	0.10	0.15	0.02	0.34	0.15	1.2E+04	39.89
FC5	cascade	Jun 2008	11.87	0.163	0.20	0.13	1.15	0.50	0.83	0.03	0.09	0.60	0.12	0.48	0.45	6.6E+04	4.64
		Jul 2008	11.89	0.163	0.10	0.08	0.94	0.62	0.98	0.03	0.09	0.24	0.02	0.37	0.23	1.6E+04	17.64
		Jul 2007	12.80	0.159	0.09	0.08	0.91	0.59	0.69	0.03	0.09	0.23	0.02	0.36	0.23	1.5E+04	18.12
		Aug 2007	14.24	0.143	0.05	0.05	0.74	0.24	0.74	0.03	0.09	0.12	0.01	0.28	0.16	5.5E+03	39.22
FC6	cascade	Jun 2008	19.06	0.195	0.17	0.12	1.07	0.39	1.33	0.05	0.09	0.61	0.10	0.48	0.48	6.2E+04	4.73
		Jul 2008	20.61	0.181	0.09	0.07	0.92	0.38	1.59	0.05	0.09	0.23	0.02	0.36	0.24	1.5E+04	19.33
		Jul 2007	19.38	0.185	0.09	0.07	0.91	0.49	2.33	0.05	0.09	0.27	0.02	0.37	0.27	1.8E+04	15.29
		Aug 2007	22.11	0.166	0.04	0.05	0.67	0.36	1.71	0.05	0.09	0.13	0.01	0.28	0.17	5.7E+03	36.16

[a] L_r is average reach length (m); W is average wetted width (m); H is step height; L_s is step length from step lip to step lip; u^* is shear velocity ($\sqrt{ghS_0}$) (m); Re is Reynolds number; Fr is Froude number.

dent variables that were significant in the regressions for each channel type. The R_h/D_{84} was thought to be an appropriate measure of both the variation in flow and the roughness created by larger grains in a channel and was found to be a more appropriate measure of explaining the variability in total flow resistance in cascade reaches, A more appropriate relative submergence control variable in step-pool reaches is R_h/H. The significance of R_h/D_{84} in cascade reaches is most likely related to the dominance of grain resistance in these reaches, whereas R_h/H better represents spill and form resistance in step-pool reaches.

[66] Wood load is also a significant explanatory variable, particularly when combined with S_0 and flow period or q^*. There is some correlation between wood load and S_0, but

overall the variable wood load seems to represent both form drag and spill resistance that is related to the amount of wood in each reach [*Curran and Wohl*, 2003; *Comiti et al.*, 2008]. The total wood load explains more of the variability in f in cascade reaches, most likely because there is much larger variation in wood load in these reaches versus step-pool reaches.

[67] Channel type is a significant explanatory variable only if flow period, q^*, and S_0 are held constant in the regression. Therefore, at particular flows and S_0 there are significant differences between step-pool and cascade reaches. The overall values of total f in step-pool reaches were higher than in cascade reaches for a given S_0 and flow period. The plane-bed reach was consistently different from all other channel types. These differences suggest that each channel type may need to be accounted for separately when developing equations to predict f. The interrelationship between S_0, D_{84}, H/L, wood load, and channel type means that S_0 may be able to be used to remotely determine channel features. Further work should be done to consider if separate resistance equations could then be applied to those channel types, determined from remote data.

[68] Returning to our original, most general hypothesis that predictable patterns of relative magnitude of total resistance exist throughout a channel network and that simple variables such as gradient can be used to predict these patterns, we conclude that gradient is a useful predictor of spatial variations in flow resistance at a given time (i.e., when flow varies only spatially as a function of drainage area). Spatial and temporal variations in resistance are more effectively predicted by combining gradient with q^* or flow period.

Appendix A

[69] Over the course of two summers, 59 data points were gathered in Fraser Experimental Forest, including channel geometry and hydraulic data (Table A1). The data listed in Table A1 were used for the statistical analysis described above. The values of friction factor and other channel geometric data are shown for individual discharges, unlike Table 2, which shows the range of values collected in each reach.

[70] **Acknowledgments.** This research was funded by the Hydrologic Sciences Program of the National Science Foundation (EAR 0608918). The USDA Forest Service Rocky Mountain Research Station and field assistants Mark Hussey, Dan Dolan, Alexandra David, Lina Polvi, and Dan Cadol provided logistical support. The comments of Alain Recking and two anonymous reviewers helped us to refine the paper.

References

Aberle, J., and G. M. Smart (2003), The influence of roughness structure on flow resistance on steep slopes, *J. Hydraul. Res.*, *41*, 259–269.

Abrahams, A. D., G. Li, and J. F. Atkinson (1995), Step-pool streams: Adjustment to maximum flow resistance, *Water Resour. Res.*, *31*, 2593–2602, doi:10.1029/95WR01957.

Baiamonte, G., and V. Ferro (1997), The influence of roughness geometry and Shields parameter on flow resistance in gravel-bed channels, *Earth Surf. Processes Landforms*, *22*, 759–772, doi:10.1002/(SICI)1096-9837(199708)22:8<759::AID-ESP779>3.0.CO;2-M.

Bathurst, J. C. (1982), Theoretical aspects of flow resistance, in *Gravel-Bed Rivers*, edited by R. D. Hey, J. C. Bathurst, and C. R. Thorne, pp. 443–465, John Wiley, Hoboken, N. J.

Bathurst, J. C. (1985), Flow resistance estimation in mountain rivers, *J. Hydrol. Eng.*, *111*, 625–643, doi:10.1061/(ASCE)0733-9429(1985)111:4(625).

Bathurst, J. C. (1986), Slope-area discharge gaging in mountain rivers, *J. Hydrol. Eng.*, *112*, 376–391, doi:10.1061/(ASCE)0733-9429(1986)112:5(376).

Bathurst, J. C. (1993), Flow resistance through the channel network, in *Channel Network Hydrology*, edited by K. Beven and M. J. Kikby, pp. 69–98, John Wiley, Hoboken, N. J.

Bathurst, J. C. (2002), At-a-site variation and minimum flow resistance for mountain rivers, *J. Hydrol. Amsterdam*, *269*, 11–26, doi:10.1016/S0022-1694(02)00191-9.

Bjerklie, D. M., S. L. Dingman, and C. H. Bolster (2005), Comparison of constitutive flow resistance equations based on the Manning and Chezy equations applied to natural rivers, *Water Resour. Res.*, *41*, W11502, doi:10.1029/2004WR003776.

Buffington, J. M., and D. R. Montgomery (1999), Effects of sediment supply on surface textures of gravel-bed rivers, *Water Resour. Res.*, *35*(11), 3523–3530, doi:10.1029/1999WR900232.

Calkins, D., and T. Dunne (1970), A salt tracing method for measuring channel velocities in small mountain streams, *J. Hydrol. Amsterdam*, *11*, 379–392, doi:10.1016/0022-1694(70)90003-X.

Chanson, H. (1994), *Hydraulic Design of Stepped Cascades, Channels, Weirs and Spillways*, 261 pp., Elsevier, New York.

Church, M., and A. Zimmermann (2007), Form and stability of step-pool channels: Research progress, *Water Resour. Res.*, *43*, W03415, doi:10.1029/2006WR005037.

Comiti, F., L. Mao, A. Wilcox, E. E. Wohl, and M. A. Lenzi (2007), Field-derived relationships for flow velocity and resistance in high-gradient streams, *J. Hydrol. Amsterdam*, *340*, 48–62, doi:10.1016/j.jhydrol.2007.03.021.

Comiti, F., A. Andreoli, L. Mao, and M. A. Lenzi (2008), Wood storage in three mountain streams of the Southern Andes and its hydro-morphological effects, *Earth Surf. Processes Landforms*, *33*, 244–262, doi:10.1002/esp.1541.

Comiti, F., D. Cadol, and E. Wohl (2009), Flow regimes, bed morphology and flow resistance in self-formed step-pool channels, *Water Resour. Res.*, *45*, W04424, doi:10.1029/2008WR007259.

Curran, J. H., and E. E. Wohl (2003), Large woody debris and flow resistance in step-pool channels, Cascade Range, Washington, *Geomorphology*, *51*, 141–157, doi:10.1016/S0169-555X(02)00333-1.

Einstein, H. A., and N. L. Barbarossa (1952), River channel roughness, *Trans. Am. Soc. Civ. Eng.*, *117*, 1121–1146.

Ferguson, R. I. (2007), Flow resistance equations for gravel- and boulder-bed streams, *Water Resour. Res.*, *43*, W05427, doi:10.1029/2006WR005422.

Grant, G. E., F. J. Swanson, and M. G. Wolman (1990), Pattern and origin of stepped-bed morphology in high-gradient streams, Western Cascades, Oregon, *Geol. Soc. Am. Bull.*, *102*, 340–352, doi:10.1130/0016-7606(1990)102<0340:PAOOSB>2.3.CO;2.

Hygelund, B., and M. Manga (2003), Field measurements of drag coefficients for model large woody debris, *Geomorphology*, *51*, 175–185, doi:10.1016/S0169-555X(02)00335-5.

Jarrett, R. D. (1984), Hydraulics of high-gradient rivers, *J. Hydraul. Eng.*, *110*, 1519–1539, doi:10.1061/(ASCE)0733-9429(1984)110:11(1519).

Jongman, R. H., C. F. J. ter Braak, and O. F. R. Van Tongeren (1995), *Data Analysis in Community and Landscape Ecology*, 279 pp., Cambridge Univ. Press, Cambridge, U.K.

Katul, G., P. Wiberg, J. Albertson, and G. Hornberger (2002), A mixing layer theory for flow resistance in shallow streams, *Water Resour. Res.*, *38*(11), 1250, doi:10.1029/2001WR000817.

Kean, J. W., and J. D. Smith (2006), Form drag in rivers due to small-scale natural topographic features: 2. Irregular sequences, *J. Geophys. Res.*, *111*, F04010, doi:10.1029/2006JF000490.

Keulegan, G. H. (1938), Laws of turbulent flow in open channels, *J. Res. Natl. Bur. Stand. U.S.*, *21*, 707–741.

Kutner, M. H., C. J. Nachtsheim, J. Neter, and W. Li (2005), *Applied Linear Statistical Models*, 1396 pp., McGraw-Hill, Irwin, N. Y.

Lee, A. J., and R. I. Ferguson (2002), Velocity and flow resistance in step-pool streams, *Geomorphology*, *46*, 59–71, doi:10.1016/S0169-555X(02)00054-5.

Legleiter, C. J., T. L. Phelps, and E. E. Wohl (2007), Geostatistical analysis of the effects of stage and roughness on reach-scale spatial patterns of velocity and turbulence intensity, *Geomorphology*, *83*, 322–345, doi:10.1016/j.geomorph.2006.02.022.

Leica Geosystems (2008), Cyclone 5.8.1.: Comprehensive software for working with laser scan data, San Ramon, Calif.

Leopold, L. B., M. G. Wolman, and J. P. Miller (1964), *Fluvial Processes in Geomorphology*, 522 pp., Dover, Mineola, N.Y.

Manga, M., and J. W. Kirchner (2000), Stress partitioning in streams by large woody debris, *Water Resour. Res.*, *36*, 2373–2379, doi:10.1029/2000WR900153.

Manners, R. B., M. W. Doyle, and M. J. Small (2007), Structure and hydraulics of natural woody debris jams, *Water Resour. Res.*, *43*, W06432, doi:10.1029/2006WR004910.

Montgomery, D. R., and J. M. Buffington (1997), Channel-reach morphology in mountain drainage basins, *Geol. Soc. Am. Bull.*, *109*, 596–611, doi:10.1130/0016-7606(1997)109<0596:CRMIMD>2.3.CO;2.

Pagliara, S., and P. Chiavaccini (2006), Flow resistance of rock chutes with protruding boulders, *J. Hydraul. Eng.*, *132*, 545–552, doi:10.1061/(ASCE)0733-9429(2006)132:6(545).

Parker, G., and A. W. Peterson (1980), Bar resistance of gravel-bed streams, *J. Hydraul. Eng.*, *106*, 1559–1573.

R Core Development Team (2007), *R: A Language and Environment for Statistical Computing*, R Found. for Stat. Comput., Vienna.

Reid, D. E., and E. J. Hickin (2008), Flow resistance in steep mountain streams, *Earth Surf. Processes Landforms*, *33*, 2211–2240, doi:10.1002/esp.1682.

Rickenmann, D. (1991), Hyperconcentrated flow and sediment transport at steep slopes, *J. Hydraul. Eng.*, *117*, 1419–1439.

Smart, D. M., M. J. Duncan, and J. M. Walsh (2002), Relatively rough flow resistance equations, *J. Hydrol. Eng.*, *128*, 568–578, doi:10.1061/(ASCE)0733-9429(2002)128:6(568).

Taylor, R. B. (1975), Geologic map of the Bottle Pass quadrangle, Grand County, Colorado, *Map GQ-1244*, scale 1:24,000, U. S. Geol. Surv., Reston, Va.

Thorne, C. R., and L. W. Zevenbergen (1985), Estimating mean velocity in mountain rivers, *J. Hydraul. Eng.*, *111*, 612–624, doi:10.1061/(ASCE)0733-9429(1985)111:4(612).

Trayler, C. R., and E. E. Wohl (2000), Seasonal changes in bed elevation in a step-pool channel, Rocky Mountains, Colorado, U.S.A., *Arct. Antarct. Alp. Res.*, *32*, 95–103, doi:10.2307/1552414.

Wiberg, P. L., and J. D. Smith (1991), Velocity distribution and bed roughness in high-gradient streams, *Water Resour. Res.*, *23*, 1471–1480, doi:10.1029/WR023i008p01471.

Wilcox, A. C., and E. E. Wohl (2007), Field measurements of three-dimensional hydraulics in step-pool channel, *Geomorphology*, *83*, 215–231, doi:10.1016/j.geomorph.2006.02.017.

Wilcox, A. C., J. M. Nelson, and E. E. Wohl (2006), Flow resistance dynamics in step-pool channels: 2. Partitioning between grain, spill, and woody debris resistance, *Water Resour. Res.*, *42*, W05419, doi:10.1029/2005WR004278.

Wohl, E. (2000), *Mountain Rivers*, *Water Resour. Monogr. Ser.*, vol. 14, 320 pp., AGU, Washington, D.C.

Wohl, E. E., and D. Merritt (2005), Prediction of mountain stream morphology, *Water Resour. Res.*, *41*, W08419, doi:10.1029/2004WR003779.

Wohl, E., and D. Merritt (2008), Reach-scale channel geometry of mountain streams, *Geomorphology*, *93*, 168–185, doi:10.1016/j.geomorph.2007.02.014.

Wohl, E. E., and D. M. Thompson (2000), Velocity characteristics along a small step-pool channel, *Earth Surf. Processes Landforms*, *25*, 353–367, doi:10.1002/(SICI)1096-9837(200004)25:4<353::AID-ESP59>3.0.CO;2-5.

Wohl, E., J. N. Kuzma, and N. E. Brown (2004), Reach-scale channel geometry of a mountain river, *Earth Surf. Processes Landforms*, *29*, 969–981, doi:10.1002/esp.1078.

Wohl, E., D. Cooper, L. Poff, F. Rahel, D. Staley, and D. Winters (2007), Assessment of stream ecosystem function and sensitivity in the Bighorn National Forest, Wyoming, *Environ. Manage. N. Y.*, *40*, 284–302, doi:10.1007/s00267-006-0168-z.

Wolman, M. G. (1954), A method for sampling coarse river-bed material, *Eos. Trans. AGU*, *35*, 951–956.

Zimmermann, A., and M. Church (2001), Channel morphology, gradient profiles and bed stresses during flood in a step-pool channel, *Geomorphology*, *40*, 311–327, doi:10.1016/S0169-555X(01)00057-5.

B. P. Bledsoe and S. E. Yochum, Department of Civil and Environmental Engineering, Colorado State University, Fort Collins, CO 80523, USA.

G. C. L. David and E. Wohl, Department of Geosciences, Colorado State University, Fort Collins, CO 80523, USA. (gcldavid@lamar.colostate.edu)